STRUCTURE — PROPERTY CORRELATIONS IN THE LEAD—TIN EUTECTIC ALLOY

by

ANIL KUMAR ARORA

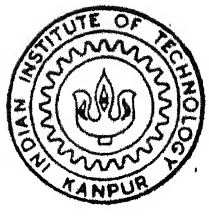

DEPARTMENT OF MATERIALS AND METALLURGICAL ENGINEERING

INDIAN INSTITUTE OF TECHNOLOGY KANPUR

November, 1993

STRUCTURE — PROPERTY CORRELATIONS IN THE LEAD—TIN EUTECTIC ALLOY

A Thesis Submitted

in Partial Fulfillment of the Requirements
for the Degree of

MASTER OF TECHNOLOGY

by

ANIL KUMAR ARORA

to the

DEPARTMENT OF MATERIALS AND METALLURGICAL ENGINEERING

INDIAN INSTITUTE OF TECHNOLOGY KANPUR

November, 1993

CERTIFICATE

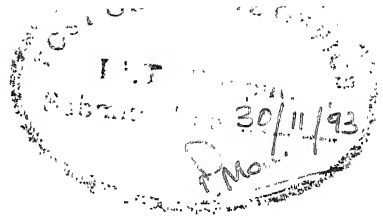

This is to certify that the work on "Structure-property correlations in the lead-tin eutectic alloy" has been carried out under our supervision and that this has not been submitted elsewhere for a degree.

(Dr. V. Bansal)

Associate Professor
Dept. of Mat. & Met. Engg.
Indian Institute of Tech.
Kanpur-208016, India

(Dr. G. S. Murty)

Professor
Dept. of Mat. & Met. Engg.
Indian Institute of Tech.
Kanpur-208016, India

ACKNOWLEDGEMENT

I wish to express my deep sense of gratitude to Dr. V. Bansal and Dr. G. S. Murty for their guidance, encouragement and genuine criticism in all phases of the present work.

I take this opportunity to express my sincere thanks to lab assistants Shri G. S. Sharma and Shri B. K. Jain for their ready assistance throughout the experimental work.

My thanks are due to Shri A. K. Jain Chief(M), CMO, SAIL for his constant encouragement and help during the course of this work. I am thankful to all my colleagues of SRM's office at Rourkela for their timely help while preparation of this thesis.

I would also like to thank my friends Anil Gupta, R. Behra, Dr. H. N. Azari, Dr. V. C. Venkatarao, B. M. Moharkar, H. K. Chauhan, V. Suresh for their constant help, support and encouragement.

I am also thankful to Shri V. P. Gupta for excellent drafting and Shri J. N. Sinku for help during typing of the thesis.

Anil Kumar Arora

CONTENTS

LIST OF FIGURES

LIST OF TABLES

ABSTRACT

Eutectic composites have been of great interest because of their several advantages over other types of composites. Eutectic composites have ease of fabrication and good thermal stability. Absence of any intermediate oxide layer between the two phases gives good interfacial bonding in eutectic composites. Mechanical behaviour of an alloy depends upon its microstructural details which in turn depend upon the processing route. In the present work, mechanical behaviour of lead-tin eutectic has been studied for different types of microstructures, evolved by different ways of processing.

The microstructures obtained in the present study are for directionally solidified, as cast and hot worked states. The lead-tin eutectic alloy has been directionally solidified at different rates of growth to get varying interlamellar spacing. Hot worked structure is obtained by swaging the cast lead-tin eutectic to two different degrees of deformation followed by annealing at 428 K for two hours in an oil bath. The specimens with these different microstructures have been tested under compression on an INSTRON machine. The compression tests were carried out at three different test temperatures (298 K, 375 K, 423 K) to study the effect of temperature on mechanical properties. The compression test was also carried out at different strain rates.

Degeneracy in the microstructure has been observed at

all speeds of directional solidification .It is observed that degeneracy in the structure increases with increasing speed of directional solidification. At lowest speed, primary dendrites of tin rich phase have been observed to grow in the direction of solidification.

Directionally solidified eutectic has shown the best strength among all types of structures at all test temperatures. The eutectic solidified with the maximum speed (191 μm/sec) exhibited the best strength at room temperature. Some strain hardening was observed in all specimens at room temperature. It is observed that directionally solidified eutectic is not highly strain rate sensitive at all test temperatures while swaged and annealed material has exhibited high strain rate sensitivity at higher temperatures.

1. INTRODUCTION

Technological developments have been constantly increasing the demand for newer materials which have better mechanical properties and high temperature properties compared to the conventional materials. These developments have come a long way by controlling the microstructures by different ways of processing and alloying additions. However, the growing needs of technological developments could not be met by controlling the microstructures alone. The constant search for newer metallic materials has rewarded the researchers with composite materials. The general approach is based on addition of a second phase having high strength by powder metallurgy or casting route. The second phase may be in the form of whiskers, fibers or particles. Composites thus developed have a very high strength with good toughness. Composites can be classified as follows:

1. Dispersion strengthened composite.
2. Particulate composite
3. Fiber composite.

In dispersion strengthened composite, second phase of fine particles, (0.01-0.1 μm dia), called dispersoids are uniformly distributed in a matrix material. Particulate composites have second phase particles (dia > 1 μm) in a ductile matrix. Fiber composites may have continuous fibers or discontinuous fibers in a ductile matrix. Continuous

fibers may be as long as structural members. Discontinuous fibers may be distributed with random orientations or aligned in one direction depending upon the way of processing. Reinforcement phases can be embedded in the matrix by different processes such as powder metallurgy route or casting route.

The other type of metallic composites which have been of great interest, to the researchers are insitu composites where reinforcement phase is evolved from the matrix itself. One example of such type of composites are eutectic alloys. Eutectic structures have been classified as divorced, degenerate, regular, complex regular, normal and faceted etc., based upon the appearance of the structure. The eutectic reaction is fundamentally a liquid to solid transformation involving a liquid of fixed composition transforming simultaneously to two solids at a constant temperature. When this reaction is carried out unidirectionally, a nearly planar solid-liquid interface is produced which gives rise to an aligned microstructure of the two solid phases. If one of the phases has a whisker like properties, the unidirectional solidification of eutectic alloys gives a practical reinforced composite material. Example: Cu-Cr eutectic alloy and Al-Ni eutectic alloy. Directionally solidified eutectic composites have some advantages compared to other types of composites. It is relatively easier to prepare composite material by the technique of directional solidification of eutectic alloys as special handling problems associated with whiskers etc. are avoided.

Another problem, which is not encountered in this type of composites is the difficulty in developing a good interfacial bond between the matrix and the reinforcement. It will allow satisfactory transfer of applied load to the constituent phases. This may be due to the fact that no intermediate oxide layers are present between the reinforcement and the matrix material since they are simultaneously produced from the melt. Eutectic composites have excellent thermal stability compared to other types of composites. This thermal stability may be related to the unique crystallographic relation that exists between the two phases.

The disadvantage of eutectic composite is the fact that the volume fraction of the high strength phase is fixed by the uniqueness of the eutectic composition. Hence, it is normally not possible to improve the properties of an eutectic alloy by changing the relative volume fractions of the eutectic mixtures. Another disadvantage is that the very high purity metals must be used to retain a planar solid-liquid interface during solidification. When relatively low purity materials are used, the planar interface breaks down to a cellular one and results in the formation of whiskers or plates that form colonies of eutectic mixtures.

Increasing growth rate of directional solidification produces increasingly finer microstructures and thereby enhances a variety of mechanical properties such as yield stress. Eutectic microstructures can have regular arrays of

lamellae or rods depending on the nature and amounts of the phases and the conditions of solidification. The rate of growth, temperature gradient at the solid -liquid interface, the velocity with which solid -liquid interface advances are the controlling parameters for the size and shape of structure. If both phases have approximately equal volume fraction, there is a preference for formation of lamellar structure (for example- Al-$CuAl_2$, Pb-Sn). If one phase is present in a small volume fraction, the phase will appear as fibrous in the matrix. The fineness of the structure i.e interlamellar spacing is determined by rate of growth that in turn determines the mechanical properties of directionally solidified eutectic alloys. So it is possible to control the mechanical properties of eutectic alloy by solidifying at different rates.

The objective of the present work is to study the effect of microstructure on mechanical properties of the lead-tin eutectic alloy. Different types of microstructures which have been evolved by different ways of processing are directionally solidified, as cast and hot worked structures. The specimens with different microstructures have been tested in compression to get stress vs strain data at three different test temperatures. The specimens have also been tested under different strain rates to see the effect of strain rate on different microstructures at three different test temperatures.

The thesis has been structured in five parts. The second chapter is literature review where directional

solidification of eutectic has been discussed along with as cast and hot worked structures. Mechanical behaviour of an eutectic has been described. The third chapter relates to the experimental set up and procedure used for the present study. The chapter on results and discussion is broadly divided into two parts. One part relates to the microstructures obtained by different ways of processing and the other part relates to mechanical testing of lead-tin eutectic alloys under different conditions. Finally, conclusions have been summarised in chapter 5.

2.LITERATURE REVIEW

Lead-Tin eutectic[1] which occurs at 61.9 wt percent tin consists of the lead rich and tin rich phases as lamellae or globules, depending on the mode of solidification. A lot of research has been done on plane front solidification of eutectic alloys. Several eutectics when directionally solidified possess fine uniform, rodlike or lamellar structures and exhibit a marked improvement in their mechanical properties. Thermal gradient and growth rate[2] are the controlling parameters to help maintain a stable planar solid-liquid interface. In polyphase alloys like eutectics, the constituents diffuse both transverse to the growing interface as well as in the growth direction and result in the observed microstructure.

2.1 LAMELLAR EUTECTIC GROWTH:

Interlamellar spacing in lamellar eutectic growth is determined by the interaction of two opposing free energy considerations[3]. One is the driving force required for transverse diffusion of solute to occur over distances comparable to the thickness of the lamellae. The other is the increased free energy associated with the area of interface boundary. The first one favours thinner lamellae as smaller driving force will be required while the second one favours thicker lamellae so as to have smaller interface boundary area per unit volume. With faster rates of freezing, the time available for diffusion is less and the re-

sultant lamellae width is less.

Theory of directional solidification of eutectic has shown[4] that interlamellar spacing, λ, varies with rate of growth as $V^{-1/2}$ where V is the rate of growth. The relation $\lambda^2 V$=constant has been verified for many systems including lead-tin eutectic[5,6,7]. Directional solidification studies of lead-tin and aluminium-copper system by Jordan and Hunt[5] have shown that the relation $\lambda^2 V$=constant has a reasonable agreement between theoretical and experimental values of $\lambda^2 V$ for a range of compositions in the lead-tin system. While in aluminium-copper system, there has been a marked variation of $\lambda^2 V$ with composition. This has been attributed to neglect of kinectic undercooling term in the theory. This term is expected to be small for a completely non-faceting system such as lead-tin and better agreement with theory for this system has been explained on this basis.

Later, Clark and Elliot[6] have reported that the interlamellar spacing(λ) is only slightly dependent on composition for lead-tin and aluminium-copper systems. The range of compositions over which an eutectic like lamellar structure is obtained was found[8] to increase with increasing values of G/V where G is the temperature gradient in the liquid and V is the growth velocity. Mollard and Flemings[9] have shown that composite structures, free of primary dendrites, can be obtained in tin-lead alloys of off-eutectic composition. It has been shown[10] that with suitable control of growth conditions, very wide compositional variations can

be tolerated while still maintaining a planar solid-liquid interface. If the interface can be maintained stable in the plane front configuration, aligned eutectic or eutecticlike structures are ob-tained. When the interface breaks down, cellular and dendritic structures are obtained. Breakdown of planar solid-liquid interface to cellular or dendritic interface has been explained by constitutional supercooling criterion. Following correlation is to be satisfied for planar solid-liquid interface growth of binary eutectics:

$$\frac{G_L}{R} \geq \frac{m_L (C_E - C_o)}{D_L}$$

where

G_L -- Temperature gradient in the liquid at the solid-liquid interface.

m_L -- Slope of the liquidus line.

D_L -- Diffusion coefficient of solute in the liquid.

R -- Rate of movement of solid-liquid interface.

C_E -- Eutectic composition.

C_o -- Starting alloy composition.

Directional solidification studies of lead-tin eutectic [11] have shown two distinct eutectic morphologies, a regular lamellar structure and a wavy lamellar structure, termed as degenerate. Figure 2.1 shows the lead-tin eutectic with degenerate and lamellar structure as reported by Verhoeven et al [11]. The grains with degenerate structure grow in

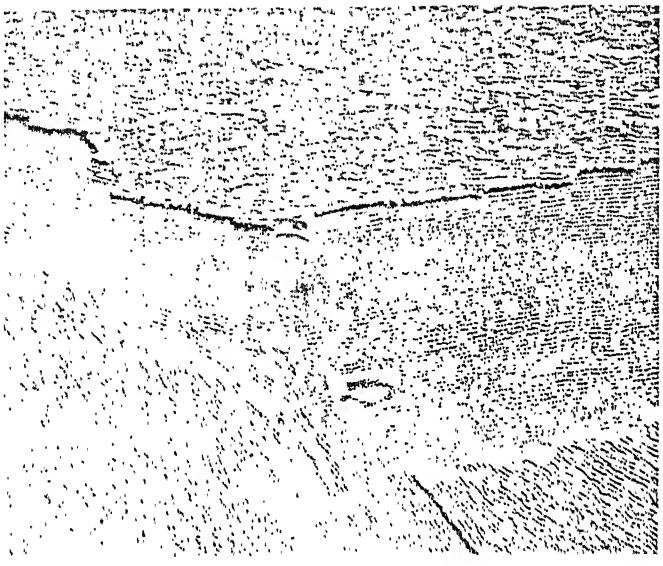

Fig 2.1: SEM micrograph of transverse section of lead-t
eutectic as electropolished. Growth rate= 41 μm/sec. Magnif
cation= 630x.

grains in directionally solidified lead-tin eutectic system at freezing rates above 83μm/sec with a temperature gradient of 3 ^{0}C/cm.

2.2 AS CAST STRUCTURE:

The lead-tin eutectic, which occurs at 61.9 wt percent tin, consists of the lead rich and tin rich phases as lamellae or globules [1], depending on the solidification rate. The higher the solidification rate, the greater is the probability of formation of a globular eutectic. The chill casting gives a globular eutectic and air cooling leads to the formation of the characteristic lamellar eutectic structure. Heat treatment at a temperature approaching that of the eutectic converts the lamellar structure to the globular form [1].

2.3 HOT WORKED STRUCTURE:

Hot working refers to deformation carried out under conditions of temperature and strain rate such that recovery processes occur substantially during the deformation process so that large strains can be achieved without much strain hardening [13]. Hot working processes are used for converting a cast ingot into a wrought product. Hot working is generally carried out above 0.5 T_m where T_m is the melting point in degrees Kelvin. For lead-tin eutectic(456 K) even the room temperature is above 0.5 T_m. Rapid diffusion at hot working temperatures, helps in decreasing the chemical inhomogeneities of the cast-ingot structure. The coarse columnar grains of the casting are broken down and refined into small equiaxed recrystallized grains.

2.4 MECHANICAL CHARACTERISTICS OF AN EUTECTIC:

The mechanical behaviour of the alloy depends on its microstructure. The microstructure of the eutectic depends on processing details and some of the types of microstructures are lamellar and equiaxed.

2.4.1 Lamellar Eutectic:

In the more conventional composite materials, reinforced by relatively large wires or fibers ($\sim 100\,\mu m$ diameter, say), much of the mechanical behaviour can be modeled quite simply by considering the load to be partitioned between the matrix and the reinforcing phases in proportion to their volume fractions. But the very fine microstructures ($\sim 1\,\mu m$ diameter), in insitu composites, lead to substantial indirect strengthening that depends upon the quality of phase alignment and the scale of the microstructures.

The simple rule of mixtures approach does not take into account the differing quality and scale of microstructures that can be produced by different processing conditions [14]. It simply partitions the stress in the ratio of the volume fractions of the constituent phases. The yield strength of the composite(σ_c) is given by the following formula.

$$\sigma_c = \sigma_\alpha V_\alpha + \sigma_\beta V_\beta$$

where

σ_α = Yield strength of α phase.

σ_β = Yield strength of β phase.

V_α = Volume fraction of α phase.

V_β = Volume fraction of β phase.

The rule of mixtures approach is based upon the concept of load sharing by the constituent phases.

Lamellar eutectics have been found to be strengthened with a decreasing interlamellar spacing[15]. In a lamellar eutectic, the yield strength (σ_{ys}) has been correlated with the spacing according to the Hall-petch equation.

$$\sigma_{ys} = \sigma_o^* + K \lambda^{-1/2}$$

where σ_o^* is a frictional stress, K is a constant and λ is the interlamellar spacing. The main argument for Hall-petch formulation is the development of dislocation pile up due to slip being blocked by the reinforcing phase[14].

Shaw[16] has reported that the yield stress (σ_{ys}) is proportional to $\lambda^{-1/2}$ for cadmium-zinc lamellar eutectic. The broken lamellar eutectics which became fibrous at higher growth rates have been reported[17,18] to show an increase in yield and ultimate strength with increasing growth rate. With further increase in growth rate, the yield and ultimate strength attain a constant value. This observation on the saturation of strength is attributed to some loss of fiber alignment at higher growth rates.

2.4.2 Superplastic behaviour of lead-tin eutectic:

Superplastic behaviour of lead-tin eutectic has been studied by several investigators[19,20,21]. Superplastic metals and alloys have high strain rate sensitivity[13]. Increasing strain rate increases tensile strength. Moreover, the strain rate dependence of strength increases with increasing temperature. Following is the relation between flow

stress and strain rate at constant temperature and strain:

$$\bar{\sigma} = K(\dot{\bar{\epsilon}})^{m}$$

where $\bar{\sigma}$ is flow stress and K is a constant. m is known as the strain rate sensitivity index. The exponent 'm' can be obtained from the slope of a plot of $\log\bar{\sigma}$ Vs $\log\dot{\bar{\epsilon}}$.

Strain rate sensitivity of metals is quite low (<0.1) at room temperature, but 'm' increases with temperature. It has been reported[20] that high strain rate sensitivity in superplastic deformation is a consequence of grain boundary sliding mechanism. The value of m >0.3 is often used as a necessary criterion for superplasticity. For lead-tin eutectic, m values have been observed to be 0.6 ± 0.1, depending upon the microstructure and test temperature. Superplastic flow in metals is characterised by extremely large plastic strains of several hundred percent[22]. The necessary conditions for the observance of superplasticity are a testing temperature greater than half the absolute melting temperature and a small equiaxed grain size, usually less than 10 μm. Such small grain sizes cannot be maintained in single phase alloys at high temperature. Ultrafine grain size can be achieved more readily in two phase alloys often with eutectic or eutectoid composition. The characteristic microstructural feature of superplastic deformation is the retention of the equiaxed grain structure throughout deformation. This observation has led to the conclusion that grain boundary sliding is the dominant deformation mechanism during superplastic flow.

3.EXPERIMENTAL PROCEDURE

3.1 ALLOY PREPARATION:

In the present work, lead-tin eutectic alloy of nominal composition 61.9 wt% tin and 38.1 wt% lead was prepared in an inert atmosphere in an existing experimental set-up. The set-up consisted of a rocking furnace, gas purification train and facility for evacuation. Lead and tin both of 99.99% purity were used. The melting point of lead -tin eutectic alloy is 456 K (fig 3.1).

3.1.1 Rocking Furnace:

It is a sixty centimeter long resistance wire wound tube furnace [23] with internal diameter of three centimeters. The furnace is held at the center of its length by two diametrically opposite horizontal pivots. It can be rocked from a vertical position down below the horizontal line through an angle of 120^{o} and can be clamped at any convenient position within an angle of approximately 30^{o} on either side of the horizontal position. One end of the furnace was closed temporarily by clamping a small piece of metallic plate. A chromel-alumel thermocouple was used to measure and control the operating temperature in the furnace.

3.1.2 Argon Purification Train:

The argon purification train basically consisted of three towers, a tube carrying copper turnings and a bubble indicator, all connected in series to commercial purity argon

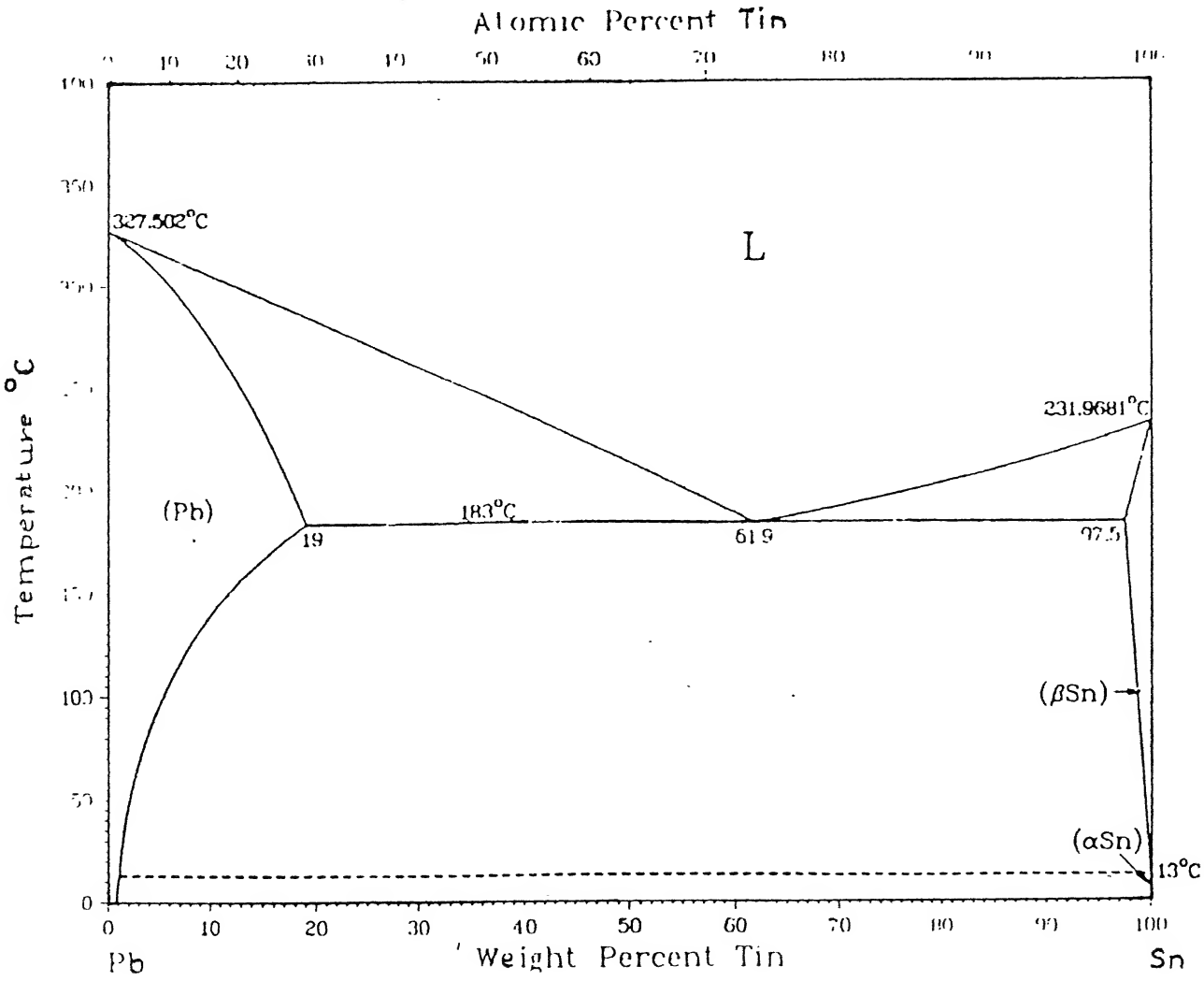

Fig. 3.1. The lead-tin equilibrium diagram.

cylinder. Fig. 3.2 gives a schematic view of the train. The first two towers, consisting of anhydrous calcium chloride and silica gel were meant to remove moisture. The third tower, containing ascarite was to remove any traces of carbon dioxide. Copper turnings were kept at 495 ^{o}C to remove any traces of oxygen. The clean gas, cooled in a condenser was supplied through a gas bubbler to the furnace. The fluid used in the gas bubbler was dibutyl phthalate.

3.1.3 Specimen Capsule:

Melting, lngot casting and finally the directional solidification was carried out in pyrex tube capsules (fig. 3.3). The capsule consisted of two parts, a bulb portion, provided for proper mixing after melting and a cylindrical portion, for casting and used for directional solidification later. The bulb portion of the capsule was cut off after each casting and was saved to be reused.

3.1.4 Alloy Making:

Specimen capsule ,containing 38.1 wt% lead and 61.9 wt% tin was kept in the rocking furnace and was connected to a rotary vacuum pump and purified argon gas supply through a two way stopcock. Initially, the capsule was evacuated and then filled with argon. This process of evacuation and back-filling was carried out several times at increasing temperatures before the charge started melting. The charge was kept at 400 ^{o}C for half an hour to ensure complete melting and then the furnace was rocked for 15-20 times to ensure proper mixing of the melt. The furnace was tilted to collect the molten alloy in the cylindrical mold of the capsule. The

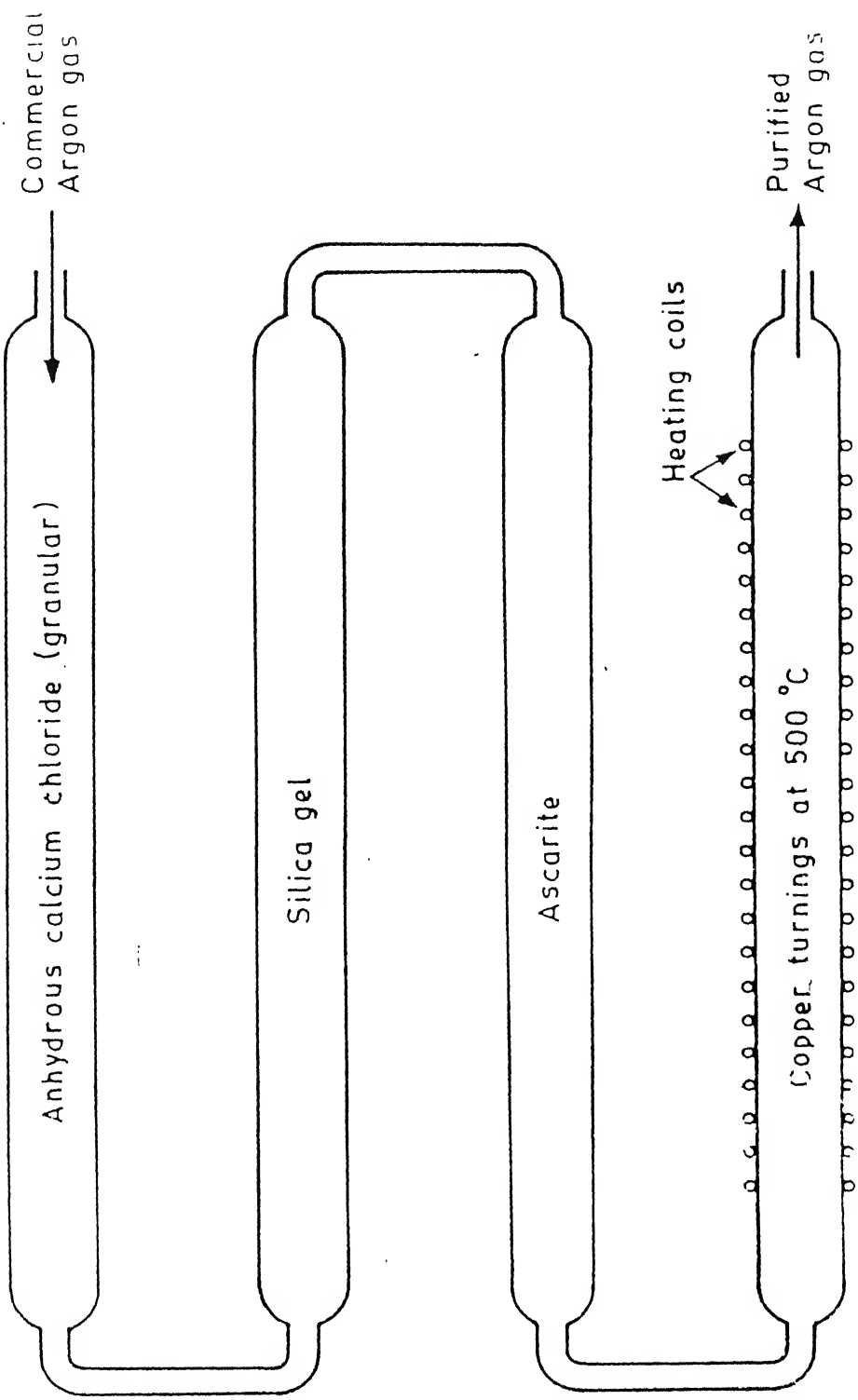

Fig. 3.2. Schematic diagram of argon purification train.

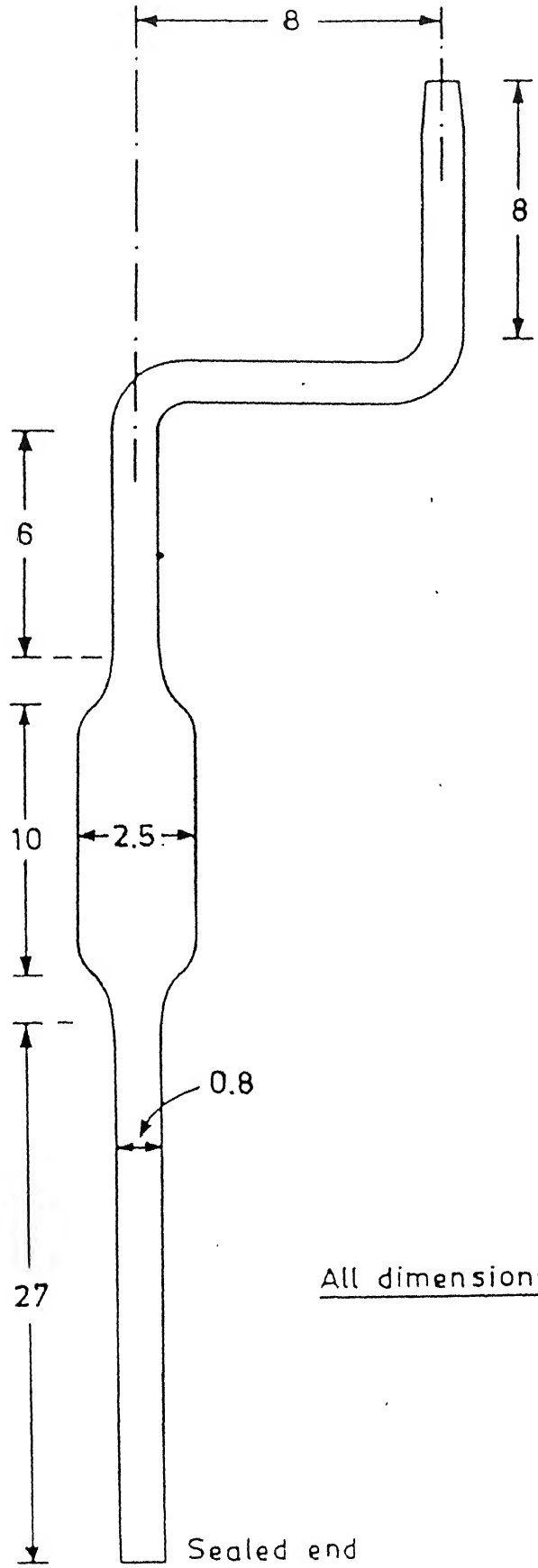

All dimensions in cm

Fig 3.3 Sch...

furnace was allowed to cool down to 250 °C before the capsule was taken out for further cooling to room temperature in the air. The cylindrical mold carrying the ingot was chopped off from the bulb portion for subsequent use in directional solidification.

3.2 DIRECTIONAL SOLIDIFICATION:

3.2.1 Directional Solidification Unit:

The eutectic alloy was solidified directionally in an existing experimental set-up. Fig 3.4 gives a schematic diagram of the apparatus used. In the apparatus, the furnace and the chill ring were moved with respect to a stationary ingot. The moving furnace and chill assembly maintained a constant thermal gradient infront of the solid -liquid interface through out the run. The furnace and chill assembly moved upward thus solidifying the ingot from bottom to the top. The drive mechanism for movement of the furnace and chill assembly is shown in the figure 3.4. The controller permitted a continuous and instantaneous change of speed of the motor. The direction of rotation of the motor was reversible so that the furnace could be moved up and down. It was ensured that the furnace moved only in a vertical line without any axial rotation.

The pyrex crucible containing the specimen sat in a blind hole in the crucible stand. The crucible was held firmly by means of three screws fitted into the wall of the blind hole. The crucible stand was made of a brass rod and mounted on a metallic base plate. The base plate was sitting

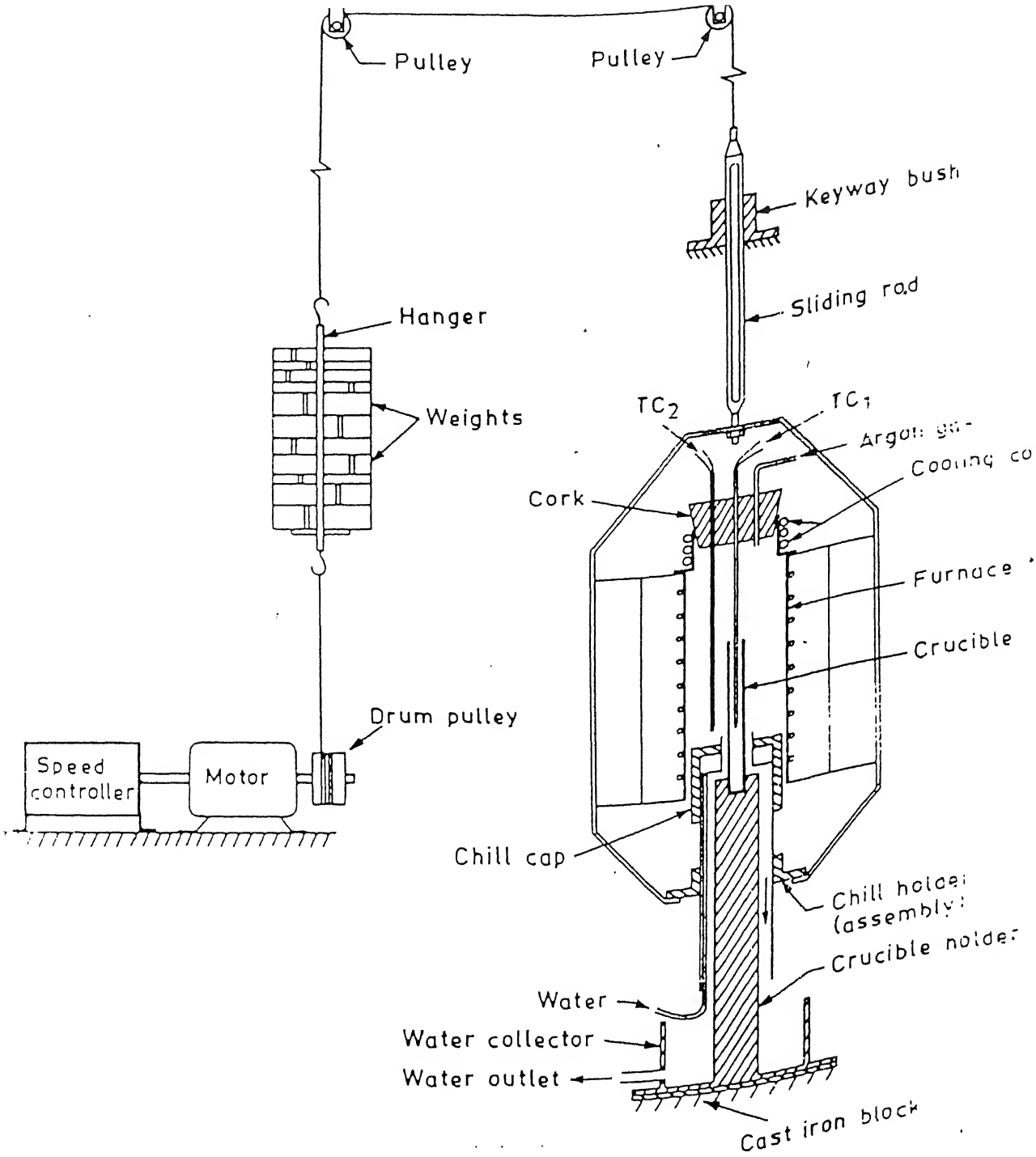

Fig. 3.4. Schematic diagram of the directional solidification setup used.

on a special cast iron block where it was screwed tightly. This is the same block as used as base for sand rammers to absorb vibrations to the crucible.

3.2.2 Directional Solidification Run:

The crucible with the solidified ingot was made to sit in the crucible stand. The thermocouple with a protective quartz sheath for determining the position of solid-liquid interface was inserted into the crucible from the top. The furnace was brought down to the lowest possible position. One index mark was there on the furnace to determine the position of the furnace using a cathetometer before start of the run and during the run. The initial position of the index mark in the cathetometer was noted down. Other parameters required for determining the position of solid-liquid interface were noted down(Appendix 1). Argon gas was supplied to the furnace at a rate of 130-150 bubbles/min. Water supply to the chill assembly was turned on at a rate of 350 ml/min. Water supply rate to the chill assembly and rate of argon gas supply were kept same in all directional solidification runs. After melting of the ingot an equilibrium was reached such that the rate of heat supply to the melt from the furnace became equal to the heat extracted by the chill ring. This condition was assumed to have been achieved when a no change in the temperature at the position of the solid-liquid interface was noted with the help of the thermocouple.

The initial position of the solid-liquid interface was determined with the help of the position of the thermocouple with its tip at the solid-liquid interface(Appendix 1). The

temperature gradient in the melt ahead of the solid-liquid interface(figure 3.5) was determined by positioning the thermocouple in the melt at different points. The tip of the thermocouple was kept one centimeter away from the solid-liquid interface during the directional solidification. The potentiometer knob of the motor speed controller was set to get a desired speed of the motor. The motor was put on and the furnace started moving upward. The position of the index mark on the furnace was noted down with the help of cathetometer for different intervals of time(Appendix 2). These readings give the actual speed of the furnace. After each run, power supply and argon supply to the furnace and water supply to the chill device were stopped. The crucible was taken out of the furnace and broken to recover the directionally solidified ingot. Typically, about 7-8 cm length at the lower end of the ingot remained unmelted because of the presence of the chill-ring. Thus, in an ingot of about 18 cm totel length, 10-11 cm upper portion was directionally solidified.

3.3 MECHANICAL WORKING:

An ingot of diameter 10.7 mm was prepared in a quartz capsule for subsequent swaging. The molten ingot was taken out of the furnace at 250 ^{o}C and quenched in water. The cast ingot was hot worked by swaging in order to break the cast structure and to get different sizes of equiaxed grains. A length of 12.0 centimeter rod was cut from the cast ingot and it was swaged to 7.6 mm diameter. The remaining part of the

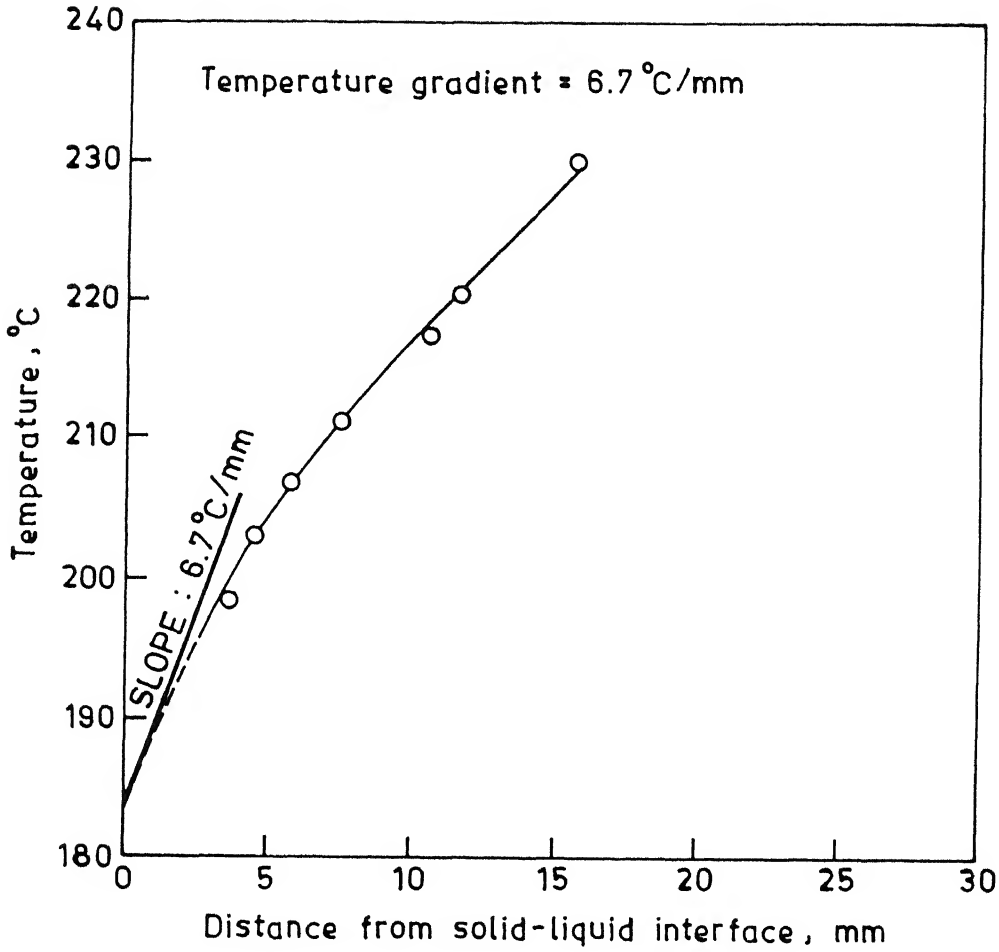

Fig. 3.5. Temperature profile near the solid-liquid interface.

cast rod was swaged to 5.6 mm diameter. As swaged rods (dia = 7.6mm and dia = 5.6mm) were annealed in a silicon oil bath at 428 K for two hours. The temperature of the oil bath was maintained within ± 2 °C.

3.4 SPECIMEN PREPARATION FOR COMPRESSION TEST:

Specimens for compression test were prepared from directionally solidified, hot worked (swaged) and as cast rods by machining on a lathe. Water cooling was used during all machining operations like turning, cutting with jeweller's saw and facing of the surfaces to prevent heating of the specimens. Compression test specimens were prepared with a length to diameter ratio in the range of 1.4-1.5.

3.5 METALLOGRAPHY:

Specimens for metallogrphic observations were cut from the rods with jeweller's saw. Transverse and longitudinal sections for directionally solidified ingots and hot worked rods were prepared.

The surfaces of the specimens to be prepared for metallography were scraped with a sharp edge of glass slide[24]. Scrapping with glass was done to avoid grinding of the surfaces on coarser emery paper which may cause distortion of the metal. The scrapped surface was polished on 4/0 emery paper in the presence of glycerol. Glycerol was used to avoid clogging of the emery paper. Thus flat surface obtained from the scrapping and polishing was dipped into concentrated hydrochloric acid for a few seconds to remove any distorted material on the surface.

Finally, the specimens were polished on a wheel with

polishing cloth, making use of fine MgO suspension. The scratch free polished samples were cleaned thoroughly first with tap water followed by distilled water. The polished surface was etched and again polished. This cycle of polishing and etching was repeated three times in each case.

The following etchant was used for etching the surface.

HCl : 2ml

HNO_3 : 5ml

Distilled water : 93ml

Final etching was done by dipping the polished surface in the etchant for 45 seconds.

3.6 MECHANICAL TESTING:

All the tests were done in compression on an Instron testing machine. These tests were done in the as cast, directionally solidified with four different speeds of directional solidification and hot worked conditions at three different test temperatures (RT:298 K, 373 K, 423 K). At room temperature, ordinary grease was used as a lubricant to minimise the friction between compression plates and end faces of the specimen. High temperature compression tests were carried out by enclosing the compression test assembly in a silicone oil bath. The oil bath was kept at the desired temperature. The temperature was maintained within $\pm$ 1 ^{o}C of the required value. The specimen was kept at the desired temperature for half an hour before start of the actual compression test. Two different types of tests were performed as described below.

(a) Constant cross-head speed test:

The specimens were compressed upto 2mm at a constant cross-head speed of 0.1mm/min. The load-time record was used to obtain true stress versus true strain data. The true stress (σ) was calculated using the formula $\sigma = S(1+e)$. Similarly the true strain was obtained from $\epsilon = \ln(1+e)$. S and e are engineering stress and engineering strain respectively.

(b) Differential strain rate test:

The tests were done to study the effect of strain rate on flow stress of different specimens at different temperatures. Step changes in cross-head speeds were made at strain intervals of 2-3%. The cross-head speeds used were 0.05,0.1,0.2,0.5,1.0,2.0 and 5.0 mm/min. The load corresponding to each of the cross-head speeds was thus recorded, from which, the true stress vs true strain rate data were calculated. The strain rate sensitivity index ($m = d\log\sigma / d\log\dot{\epsilon}$) was calculated from the relation:

$$m = \frac{\log(P_2/P_1)}{\log(V_2/V_1)}$$

P_1 and P_2 are steady state loads corresponding to cross head speeds V_1 and V_2 respectively.

4. RESULTS AND DISCUSSION

The results are divided into the observations on microstructures evolved through processing (directional solidification, casting and hot working) and the mechanical behaviour of the eutectic alloy at room and elevated temperatures. The correlation between the microstructure and mechanical behaviour is discussed.

4.1 MICROSTRUCTURES:

4.1.1 Directionally Solidified Structure:

The lead-tin eutectic was solidified unidirectionally with three different speeds (25 μm/sec, 91 μm/sec, 191 μm/sec) of solidification to get varying interlamellar spacing. The temperature gradient in the liquid was kept constant at 6.7 ^{0}C/mm. Optical micrograph of stage micrometer scale was used to get the correct magnification on optical micrographs of directionally solidified eutectic. To determine the interlamellar spacing the procedure used was as follows. A line was drawn on optical micrograph of the transverse section (normal to the direction of growth). This line was nominally at right angle to the orientation of the lamellae in the micrograph. Number of lamellae, over a certain distance was counted. This distance was measured with the help of a vernier calipers. Interlamellar spacing was determined by dividing the distance with the number of lamellae. The measured values of interlamellar spacing (λ) have been tabulated in Table 4.1 for various speeds of

TABLE 4.1

Interlamellar Spacing (λ) at Various Speeds of Directional Solidification

Growth Rate(R) ($\mu m/s$)	Temperature Gradient(G) $^{o}C/m.m$	Interlamellar Spacing λ (μm)	$\lambda^2 V$	G/R x 10^4
191	6.7	1.05	210	3.5
91	6.7	0.841	64	7.4
25	6.7	1.225	38	26.8

solidification.

The eutectic solidified with the lowest speed of 25 μm/sec (fig 4.1) shows primary dendrites surrounded by eutectic microstructures in the matrix. It can be concluded that primary dendrites are of tin rich solid solution as etching of the eutectic reveals the tin rich phase as light and the lead rich phase as dark. The primary dendrites are observed to grow in the direction of solidification (fig 4.1 b). At higher magnification, broken lamellae (also referred as degenerate [11]) are observed in between the primary dendrites (fig 4.2). Presence of primary dendrites may be due to the composition being off-eutectic. This may have arisen due to gravity segregation of lead at the lowest speed (25 μm/sec) of solidification. Pockets of lead (black spots) are observed in fig 4.1 (a) due to gravity segregation which would have left the liquid with an off-eutectic composition on tin rich side of lead-tin eutectic. In the case of directional solidification of off-eutectic composition, the growth can be maintained as plane front i.e, no primary dendrite formation, provided the following relation [10] holds.

$$G_L/R \geqslant \frac{m\,(C_L - C_E)\,C_o}{D_L}$$

where

G_L -- Temperature gradient in the liquid in front of solid-liquid interface.

R -- Rate of growth.

m -- Slope of the liquidus on the tin rich side in the

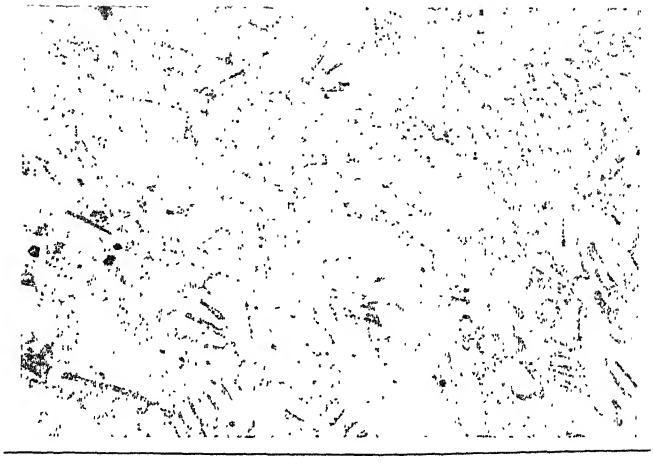

(a)

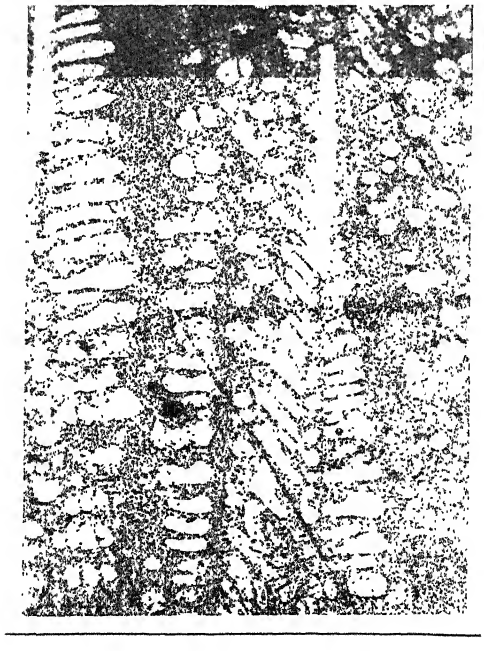

(b)

Fig 4.1: Optical micrograph of directionally solidified lead tin eutectic. Growth rate=25 μm/sec. Magnification= 100x. (a

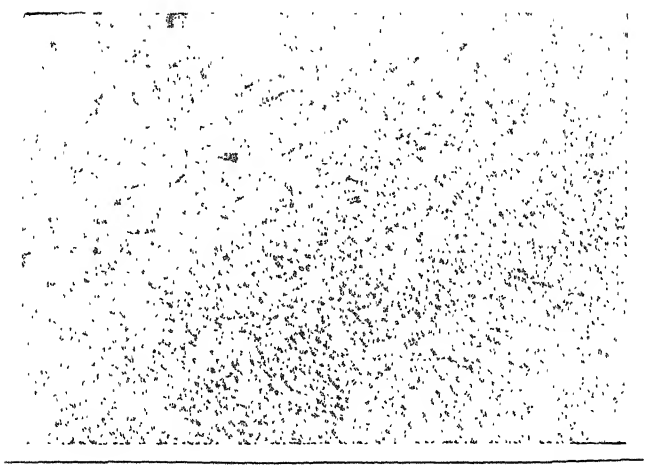

Fig 4.2: Optical micrograph of transverse section of directionally solidified lead-tin eutectic. Growth rate= .25 μm/sec. Magnification= 500x.

lead -tin equilibrium phase diagram.

C_E -- Eutectic composition.

C_o -- Composition in front of solid-liquid interface.

D_L -- Diffusivity of solute.

Following values have been used for the lead-tin system in the present work.

m_L -- 1.23 ^{O}C/wt percent tin

D_L -- 6.7×10^{-6} cm^2/sec

G_L -- 67 ^{O}C/cm

R -- 0.0025 cm/sec

In the present case, it is found that for plane front solidification, $(C_E - C_o)$ should not be greater than 0.15 wt percent. So it is assumed that due to segregation of lead, the alloy composition has deviated much more than 0.15 wt percent on the tin rich side of the eutectic. Thus it is obvious that there has been a breakdown of planar solid-liquid interface which has given rise to primary dendrite phase at the lowest speed of directional solidification.

At a higher speed of directional solidification (91 μm/sec), interlamellar spacing has become 0.841 μm which is finer (fig 4.3) than the interlamellar spacing of the eutectic solidified with 25 μm/sec. Degeneracy in the structure is observed at this speed also. The eutectic exhibits pockets of lamellar and degenerate structures. Measurements of interlamellar spacing has been made on the regular lamellar structure. Figure 2.1 shows the presence of degenerate structure in the lead-tin eutectic as reported by Verhoeven et al[11]

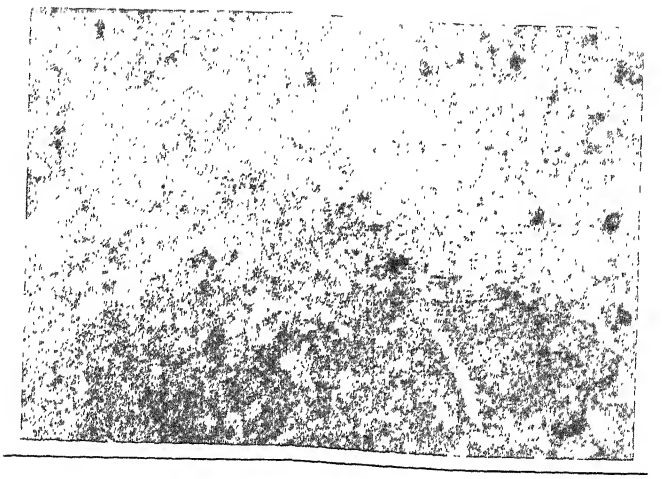

(a)

(b)

Fig 4.3: Optical micrograph of directionally solidified lead-tin eutectic. Growth rate=91 μm/sec. Magnification= 500x. (a) Transverse section (b) Longitudinal section.

erate and showed no pockets of regular lamellar structure (fig 4.4). Directionallity can be seen in the longitudinal section (fig 4.4 b). Figure 4.5 shows the difference between the structure obtained at speeds of 191 μm/sec and 91 μm/sec at higher magnification.

Table 4.1 gives the calculated values of $\lambda^2 V$ for various speeds of solidification. It is found that $\lambda^2 V$ is not constant for all speeds of solidification. The relation $\lambda^2 V$ = constant is expected to hold for a regular lamellar eutectic whereas in the present work, degeneracy in the structure has been observed at all speeds of directional solidification.

4.1.2 Cast structure:

The lead-tin eutectic was cast in a pyrex tube in inert atmosphere as described in sec 3.1. As cast rod was used for directional solidification. During directional solidification, some unmelted portion remained in as cast state. This portion was used to obtain as cast structure in metallography and as cast specimens for mechanical testing.

Figure 4.6 shows the micrograph of as cast structure. In as cast state, the structure is largely equiaxed structure. It is expected to have relatively rough or step like grain boundaries.

Grain size for as cast structure was determined by mean intercept method. Exact magnification of optical micrograph of the transverse section was determined with the help of an optical micrograph of stage micrometer scale. Lines were drawn in random directions on optical micrographs.

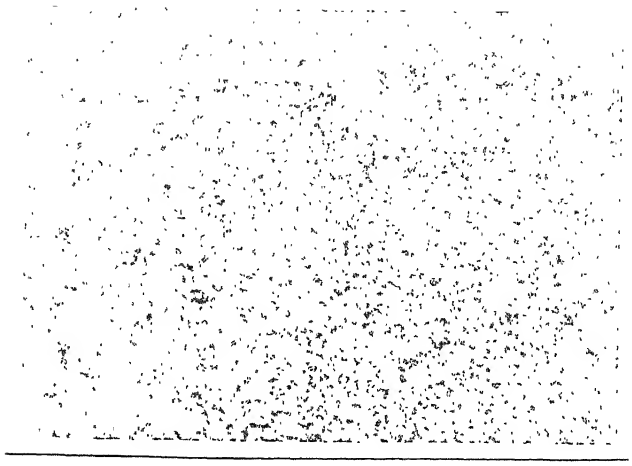

(a)

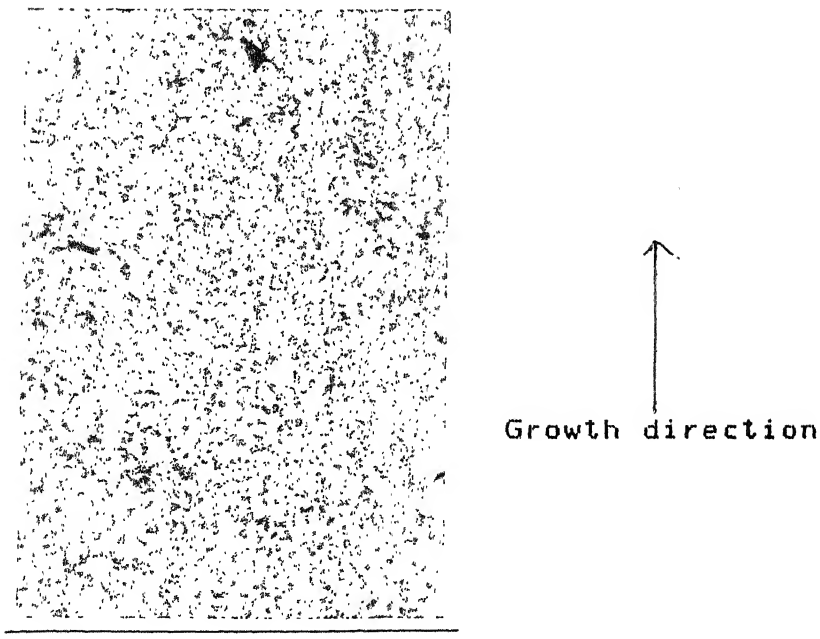

(b)

Fig 4.4: Optical micrograph of directionally solidified lead-tin eutectic. Growth rate=191μm/sec. Magnification= 500x. (a) Transverse section (b) Longitudinal section.

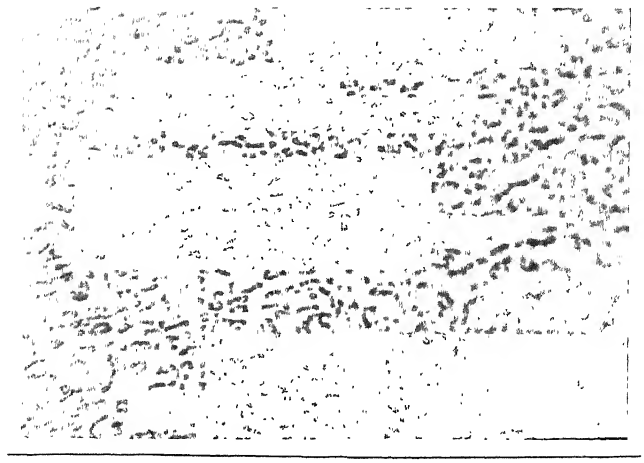

(a)

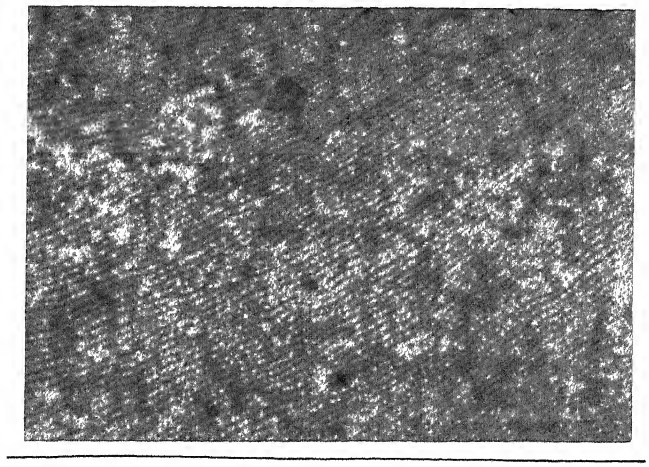

(b)

Fig 4.5: Optical micrograph of directionally solidified lead-tin eutectic. Magnification= 1000x. (a) Transverse section, growth rate= 191 μm/sec (b) Transverse section, growth rate= 91 μm/sec.

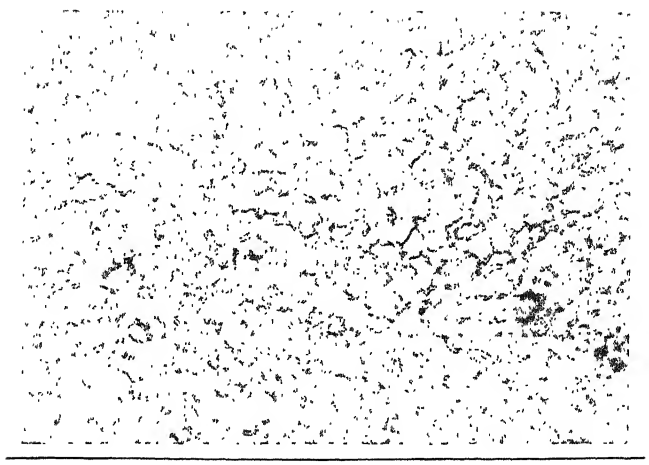

Fig 4.6: Optical micrograph of transverse section of as cast lead-tin eutectic. Magnification= 500x.

Numbers of phase boundary intersection on these lines were counted. Total length of these lines divided by number of intersection, gives grain size (mean intercept length) of as cast eutectic as 4.2 μm.

4.1.3 Hot worked structure:

Cast eutectic ingot was swaged to two different degrees of deformation (49.5 % RA and 72.6 % RA). It was subsequently annealed in an oil bath at 428 K for two hours. The structures thus obtained have been shown in figs 4.7 and 4.8 respectively. Hot working of the alloy has broken the dendritic structure and subsequent annealing at 428 K has given rise to equiaxed grains. With increasing amount of reduction in hot working, greater degree of uniformity in the microstructure is expected. Grain boundaries are expected to be smoother than in as cast state. Swaged material was not fully recrystallised during annealing as the elongated grains formed during hot working can be seen in longitudinal section in the form of mildly aligned grains (fig 4.8 b). A comparison of the transverse micrographs of the as cast structure (fig 4.6) and those for the swaged and annealed structures (figs 4.7 and 4.8) shows that with greater degree of swaging, the tin rich phase is showing greater contiguousness.

Grain sizes for swaged and annealed material were determined by mean intercept method as described above for as cast structure. Swaged and annealed material with 49.5 % RA has grain size of 5.2 μm and with 72.6 % RA has grain size of 5.5 μm.

4.1.4 Pure metals:

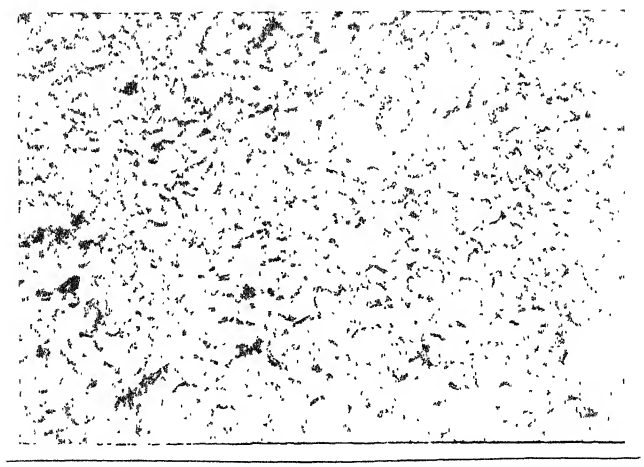

(a)

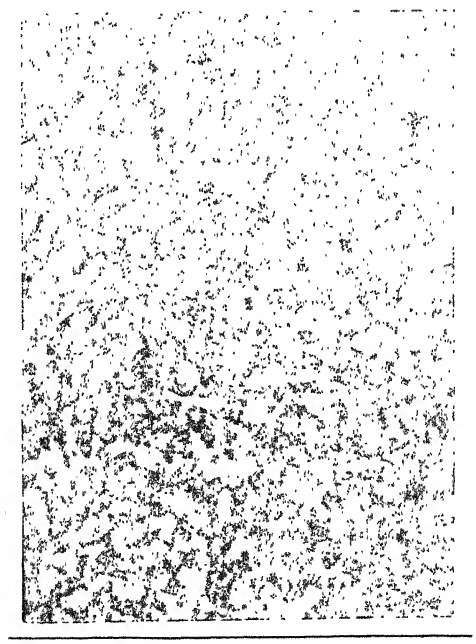

(b)

Fig 4.7: Optical micrograph of swaged (49.5% RA) and annealed lead-tin eutectic. Magnification= 500x. (a) Transverse section (b) Longitudinal section.

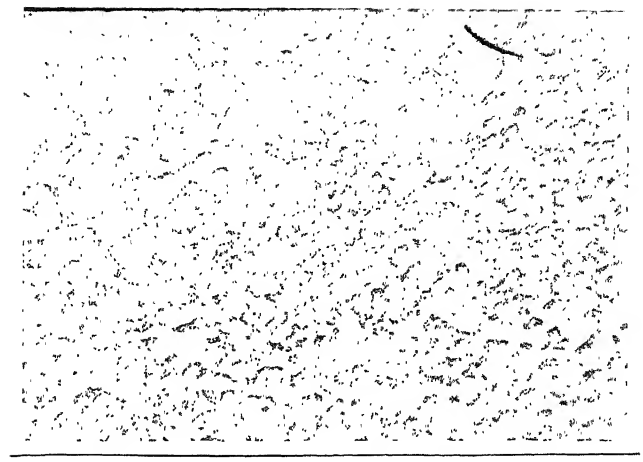

(a)

(b)

Fig 4.8: Optical micrograph of swaged (72.6% RA) and annealed lead-tin eutectic. Magnification= 500x. (a) Transverse section (b) Longitudinal section.

Pure lead and pure tin were cast in the capsule (as shown in fig 3.3) using the rocking furnace. Pure metals were melted in the furnace and the furnace was tilted to collect the molten metal in the capsule. The molten metal was allowed to solidify in the air. As cast pure lead and pure tin were annealed at 423 K for two hours in the rocking furnace. Grain sizes for lead and tin were determined with an optical microscope using an engraved square grid. Dimension of a small square of the grid was determined by using a stage micrometer scale. Number of grains in a certain area of the grid under microscope were counted. The the area of a single grain assumed to be square shaped was calculated. Square root of the area calculated gives the grain size of lead as 69 μm and grain size of tin as 97 μm.

4.2 MECHANICAL TESTING:

Directionally solidified eutectic with various speeds of directional solidification, as cast eutectic, hot worked eutectic and pure lead and pure tin were tested in compression on an Instron machine. Specimens were tested by constant cross-head speed and strain rate change tests at three different temperatures (RT:298 K, 373 K, 423 K). It is of interest to note that the melting point of lead-tin eutectic is 456 K and the homologous temperatures (ratio of test temperature to melting point in Kelvin) corresponding to three test temperatures are 0.65,0.82 and 0.93. Thus all the test temperatures are above 0.5 T_m where T_m is melting point of the eutectic in Kelvin. It may be noted that in the elevated

temperature deformation the operative mechanisms are based on dislocation controlled flow, grain boundary sliding and diffusional flow.

4.2.1 Constant cross-head speed test:

Making use of compression test data, true stress Vs true plastic strain curves have been obtained for directionally solidified, as cast eutectic, hot worked eutectic, pure lead and pure tin (figs 4.9 to 4.13) at three different test temperatures. At room temperature (298 K), directionally solidified eutectic with the highest speed of solidification exhibits the best strength among all directionally solidified specimens at various speeds. Increasing speed of directional solidification produces increasingly finer interlamellar spacing. Finer interlamellar spacing produces more number of grain boundaries which inhibit the movement of dislocations at room temperature. The variation in yield strength with interlamellar spacing can be considered in terms of Hall-petch relationship (Table 4.2). The yield strength of the eutectic is also calculated by the rule of mixtures.

In lead-tin eutectic, the volume fraction of lead rich (V_β) phase is 0.37. The calculated yield strength of lead-tin eutectic by rule of mixtures is 7.3 MPa which is much less than the experimental value. This difference may be because of: (i) the yield strength values of pure lead and pure tin have been considered instead of lead rich and tin rich phases as present in the eutectic and (ii) the yield strength values of pure lead and pure tin have been considered in as cast state. The data for aligned grain structure of these pure

TABLE 4.2

Interlamellar Spacing (λ) vs Yield Strength (σ_{YS}) Data at Various Speeds of Directional Solidification

Growth Rate(R) ($\mu m/s$)	Interlamellar Spacing (μm)	Yield Strength σ_{YS} (MPa)	$\lambda^{-1/2}$
191	1.05	36	0.976
91	0.841	33	1.09
25	1.225	32	0.904

materials would have predicted higher strengths for the directionally solidified eutectic.

At room temperature (fig. 4.9), the eutectic in the as cast state has a strength level in between the directionally solidified and hot worked materials. Though the grain size of as cast material is not much different from swaged and annealed material, it has shown a better strength than swaged and annealed material. This may be attributed to various factors such as the mixed structure (lamellar and equiaxed) in as cast state, microsegregation and grain boundary ledges. The grain boundary sliding being the expected mode of deformation in fine grained alloy at elevated temperatures (above 0.5 T_m), irregular grain boundaries with ledges are likely to exhibit greater resistance for plastic flow. On the other hand, swaged and annealed material with a more homogeneous structure and smoother grain boundaries would be expected to exhibit lesser resistance for grain boundary sliding and thereby lower strength. Another reason may be that the as cast eutectic was not annealed while hot worked eutectic was annealed at 428 K for two hours in an oil bath. Swaged and annealed material with less reduction has a slightly higher strength as compared to the material swaged to 72.7% RA. This may be considered in terms of differences in their grain size and homogeneity of their microstructure. The hot worked material with smaller grain size is showing a better strength because the grain boundaries inhibit the movement of dislocations. On the other hand, grain boundaries may weaken the

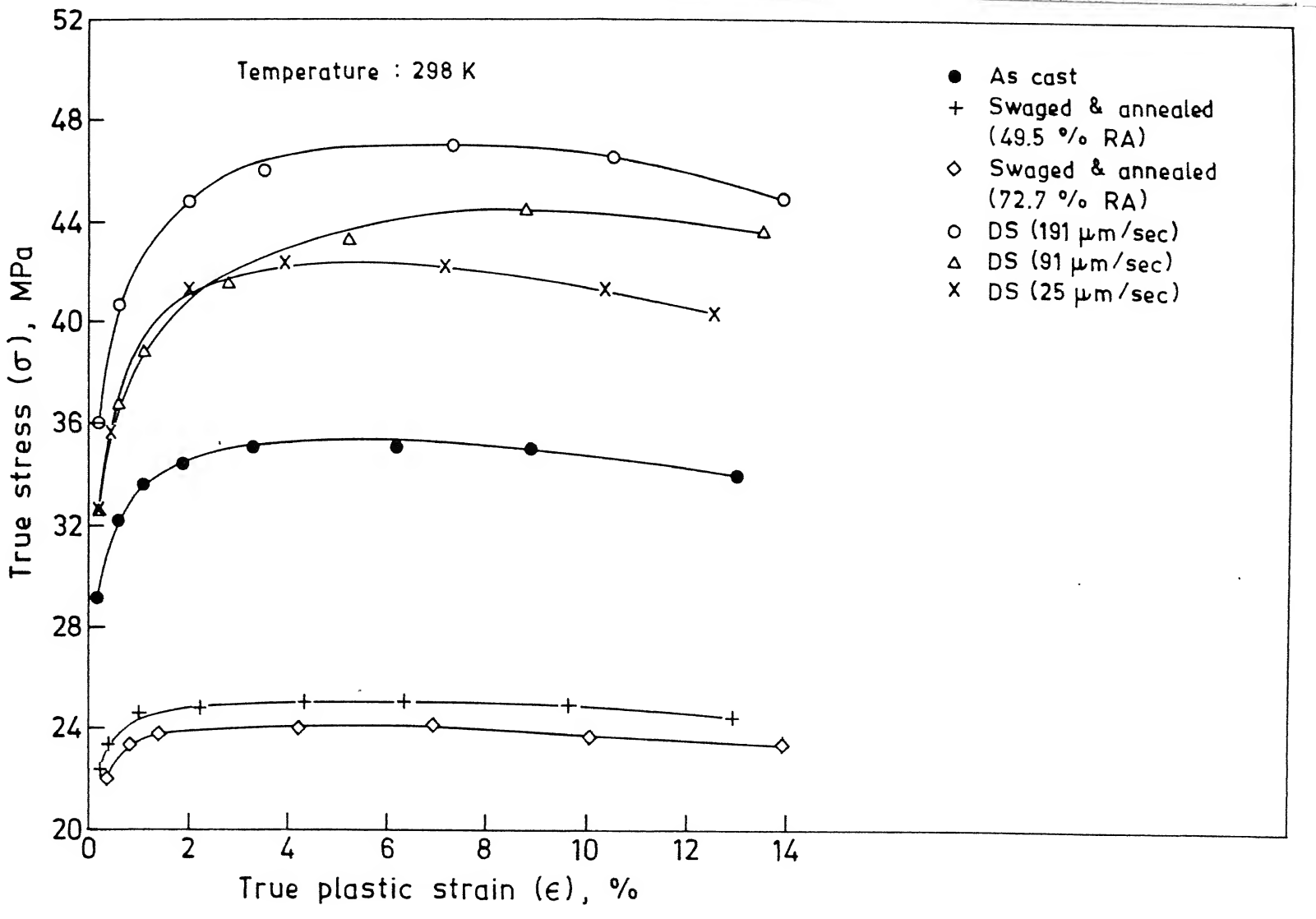

Fig. 4.9. True stress (σ) vs true strain (ϵ) curves at 298 K.
(DS = Directionally solidified) (RA = Reduction in Area)

material through a change in mechanism to grain boundary sliding. However, the grain size difference is small between the swaged and annealed eutectic with two different degrees of deformation and accordingly the difference in their strength levels is not too significant.

At higher test temperatures, strengths of directionally solidified material with different speeds of solidification lies in a narrow band (figs 4.10,4.11). The concept of rule of mixtures may be valid for a lamellar structure at higher temperature. Rule of mixtures approach determines the strength based on the volume fractions of the constituent phases. The load transfer to both the phases and thus the load sharing determines the strength of the alloy. As volume fractions of lead rich and tin rich phases are same in all directionally solidified eutectic specimens with different speeds of solidification, the strength of all the lamellar structures is expected to be independent of interlamellar spacing. Application of rule of mixtures approach, using yield strength of pure lead and pure tin at 423 K gives the strength value of 2.1 MPa for the eutectic. This is much less than the experimental value ($\sim$ 14.0 MPa) at 423 K. It is due to the equiaxed structure of pure lead and pure tin and coarser grain size of lead and tin. Instead of taking yield strengths of solid solution of lead rich and tin rich phases, pure lead and pure tin have been considered.

As cast eutectic has a strength level in between the directionally solidified eutectic and swaged and annealed eutectic at higher temperatures. This can be explained in the

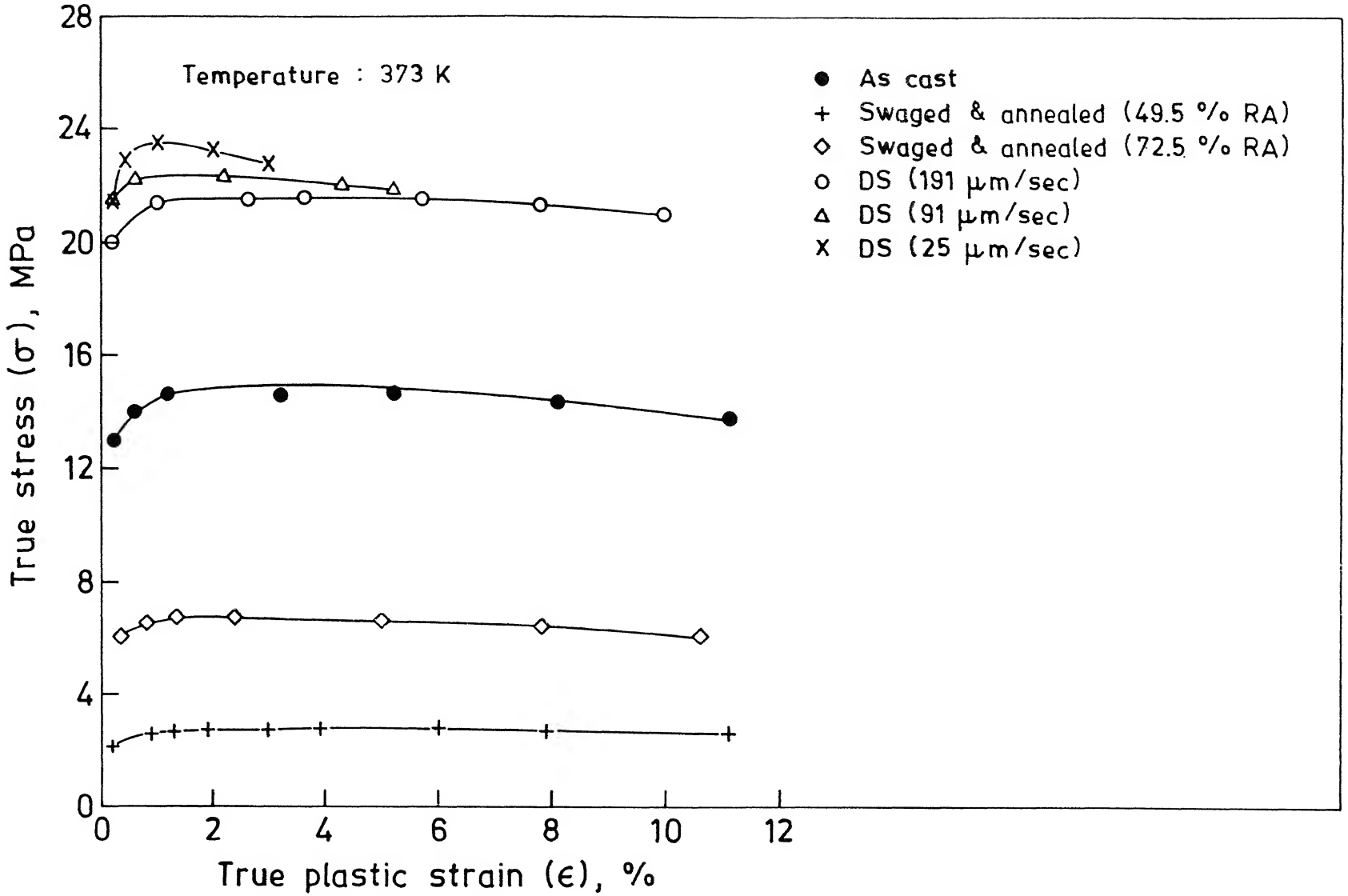

Fig. 4.10. True stress (σ) vs true strain (ϵ) curves at 373 K. (DS = Directionally solidified)

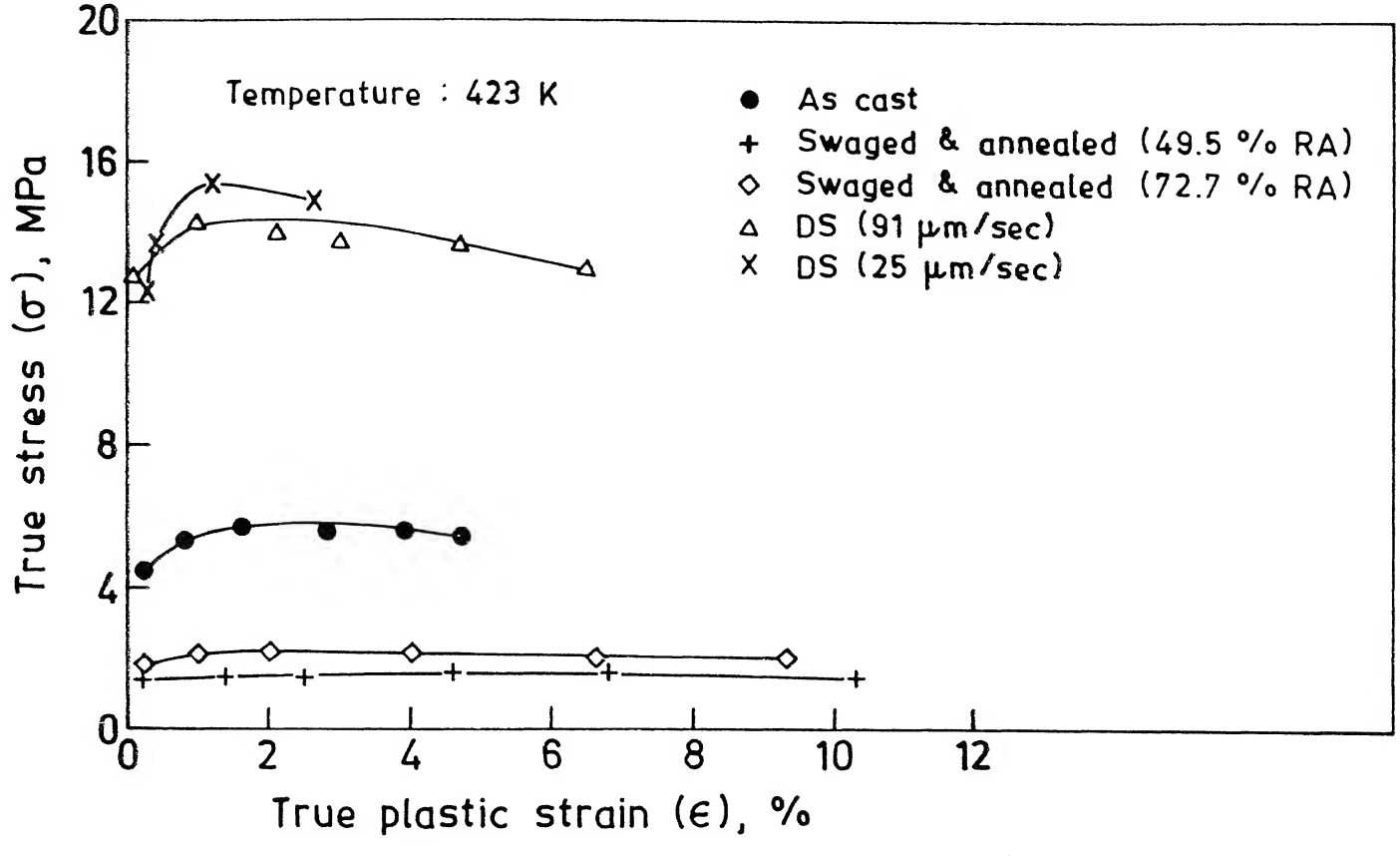

Fig. 4.11. True stress (σ) vs true strain (ϵ) curves at 423 K. (DS = Directionally solidified)

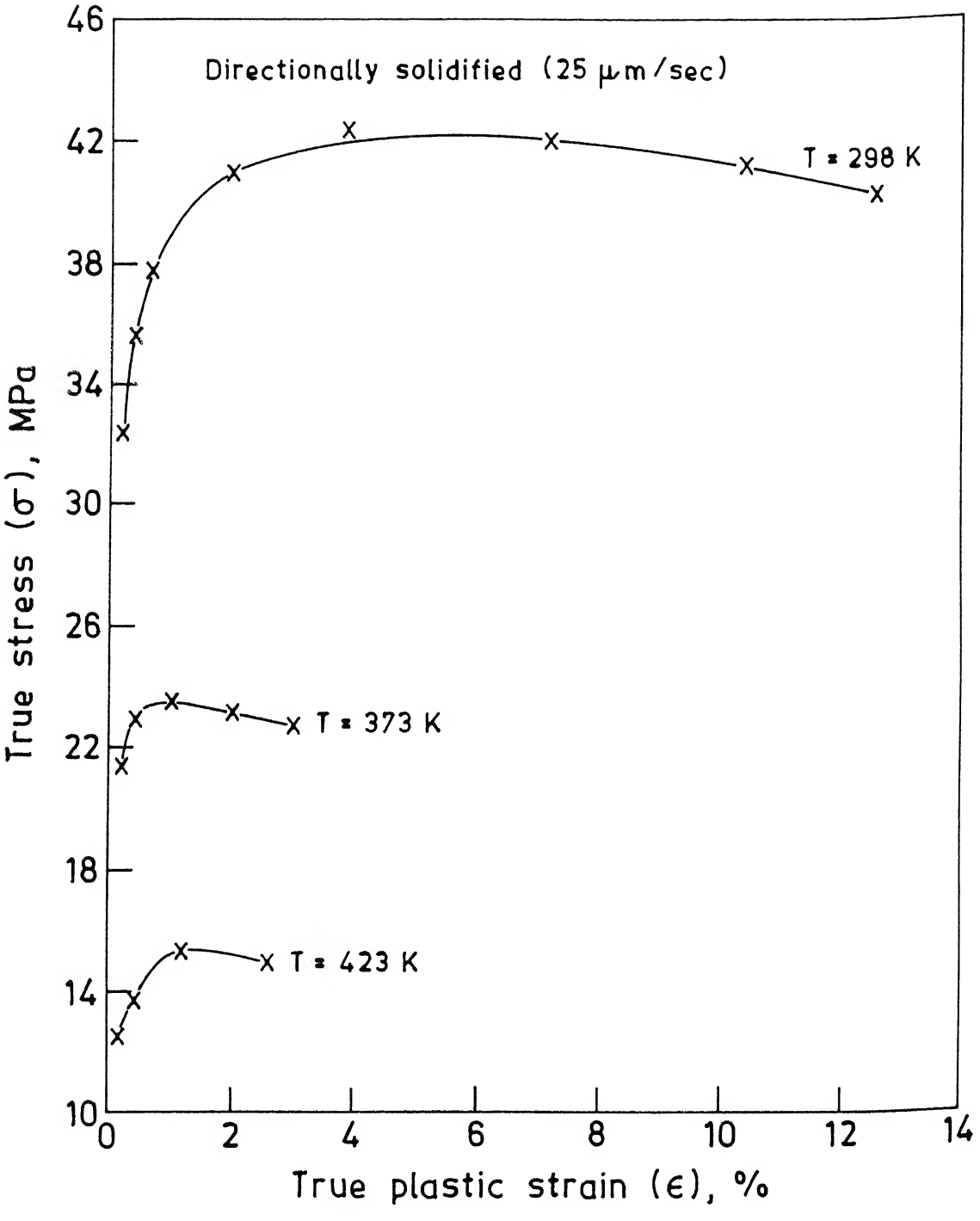

Fig. 4.12. Effect of temperature on true stress (σ) vs true strain (ϵ) curves for directionally solidified lead-tin eutectic. Growth rate = 25 μm/sec.

same way as at room temperature.

Swaged and annealed material has minimum strength level. This can be attributed to the homogenised equiaxed structure of these samples with smooth grain boundaries. Grain boundary sliding, being the important mode of plastic flow in fine grained materials, the flow stress becomes lower.

Directionally solidified eutectic shows a higher strength as compared to as cast and swaged and annealed eutectic at all temperatures. The lamellar structure of the directionally solidified material where the grain boundaries are aligned parallel to the direction of solidification, is not favourable for grain boundary sliding mechanism to operate. For the directionally solidified specimens, increasing plastic strain has resulted in a decrease in the flow stress due to softening of the material (fig 4.12). The softening was found to occur at lower plastic strains at higher test temperatures. This may be due to the instability of lamellar structure because of higher degree of deformation at elevated temperatures. Table 4.3 shows that yield strength decreases with increasing temperature for all microstructures. Directionally solidified eutectic shows higher strength than other microstructures at all temperatures. Drop in strength with increasing temperature is less in directionally solidified material as compared to drop in as cast and swaged and annealed eutectic. Table 4.4 gives peak compression strength for different microstructures at different temperatures.

TABLE 4.3

Yield Strength vs Temperature Data For Different Microstructures

Temperature (Kelvin)	Yield Strength σ_{ys} (MPa) DS (91 μm/sec)	As Cast	S & A (49.5% RA)
298	33	29	22
373	21	13	2.1
423	13	4.5	1.4

TABLE 4.4

Peak Compression Strength vs Temperature Data For Different Microstructures

Temperature (Kelvin)	Peak Strength σ_{VCS} (MPa) DS (91 μm/sec)	As Cast	S & A (49.5% RA)
298	44	35	25
373	22	15	2.8
423	14	5.7	1.6

Comparison of Table 4.3 and Table 4.4 shows that strain hardening is more at room temperature than at higher temperatures. Directionally solidified eutectic gets more strain hardened than other microstructures at 298 K (fig 4.9).

Figure 4.13 gives the stress-strain curves for pure lead and pure tin for the purpose of comparing them with those of the eutectic alloy. At room temperature, stress-strain curve for lead does not show any softening of the material as reported in the literature [22]. At higher temperatures, stress-strain curves exhibit a cyclic behaviour for lead and tin. This suggests the operation of the process of dynamic recrystallization along with strain hardening at these temperatures.

4.2.2 Differential strain rate test:

The strain rate change test was carried out in compression by changing the speed of cross-head stepwise. The cross-head speeds used were 0.05,0.1,0.2,0.5,1.0,2.0 and 5.0 mm/min. The strain rate sensitivity index ($m = d\log\sigma / d\log\dot{\varepsilon}$) was calculated.

The results of the differential strain rate test are presented in the form of stress vs strain rate plots and the strain rate sensitivity index vs strain rate plots.

At room temperature (298 K), flow stress vs strain rate curves show that flow stress increases with increasing strain rate (fig 4.14). The increase in flow stress for directionally solidified eutectic is less compared to as cast and swaged and annealed eutectic. Comparing the corresponding m values from figure 4.15, the strain rate sensitivity index

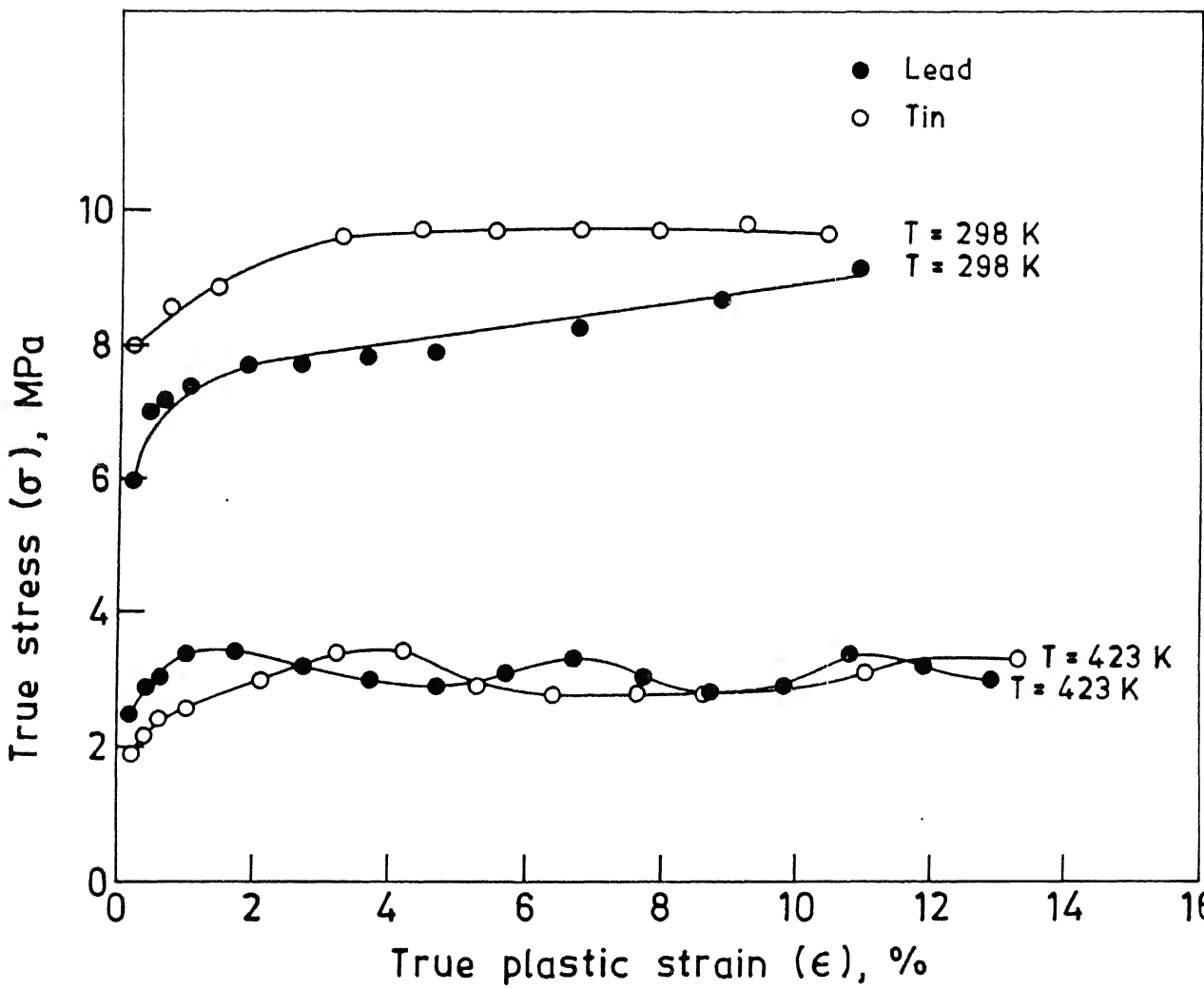

Fig. 4.13. True stress (σ) vs true strain (ϵ) curves for lead and and tin .

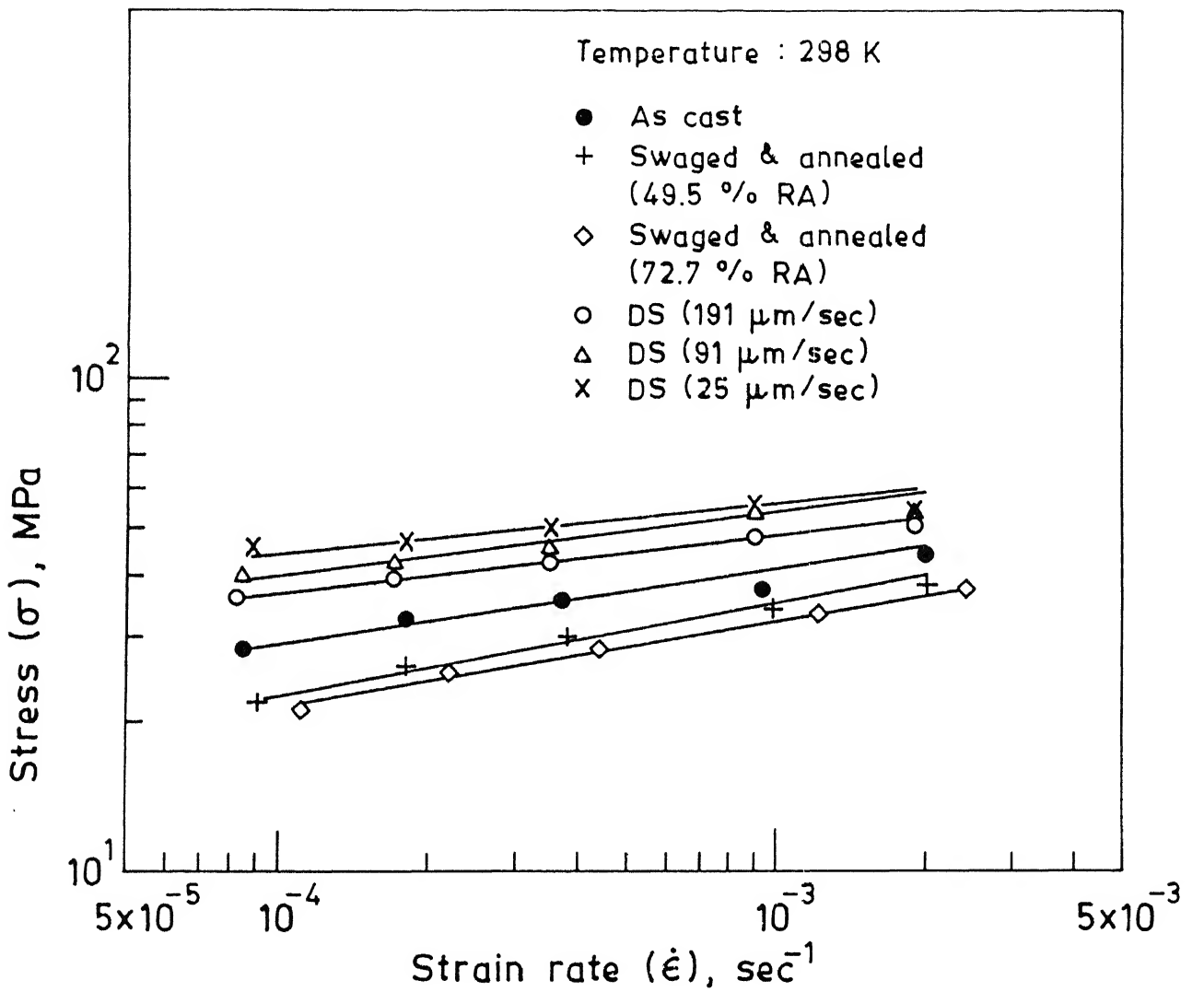

Fig. 4.14. Stress (σ) vs strain rate ($\dot{\epsilon}$) curves at 298 K. (DS = Directionally solidified)

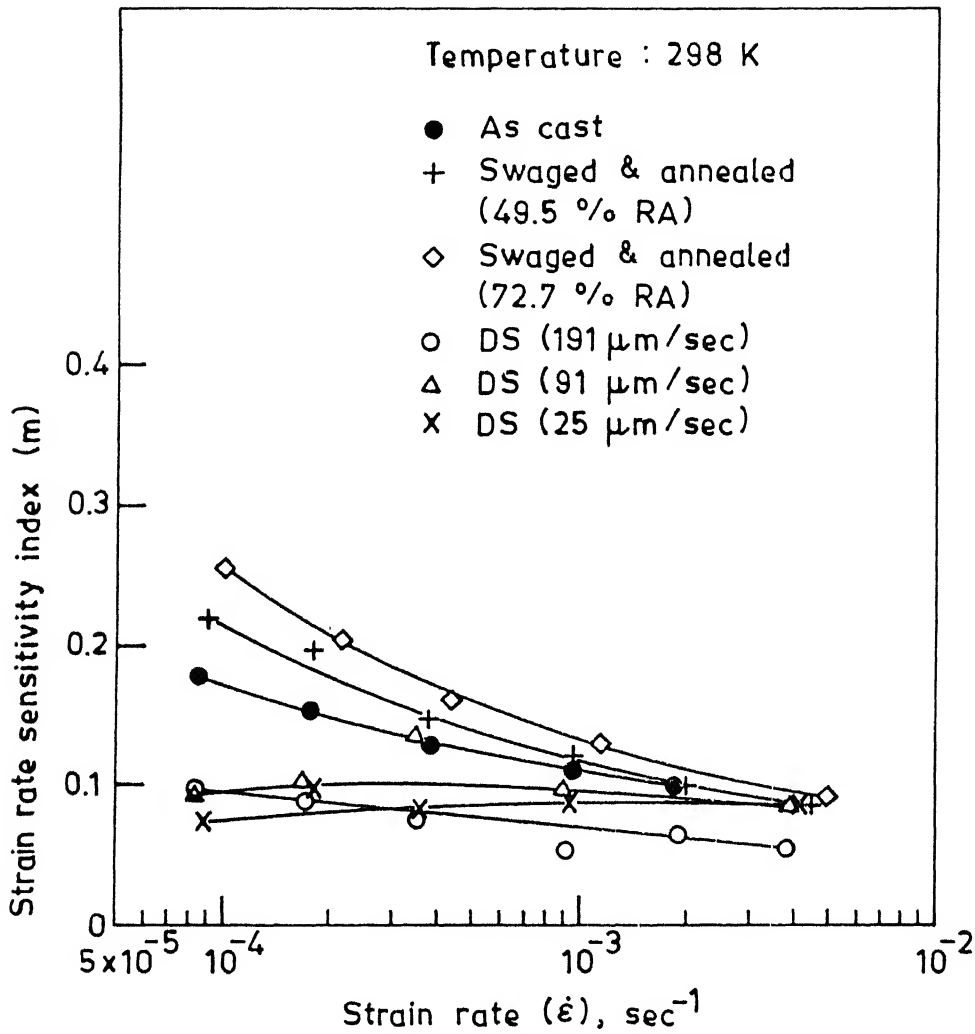

Fig. 4.15. Influence of strain rate ($\dot{\varepsilon}$) on strain rate sensitivity index (m) at 298 K. (DS = Directionally solidified)

is nearly constant for directionally solidified material at all strain rates. The m values are less than ~0.25. It shows that for directionally solidified eutectic, the mode of deformation at room temperature is not the grain boundary sliding which has a higher rate sensitivity. Deformation is mainly due to direct dislocation mechanism.

The strain rate sensitivity for swaged and annealed eutectic decreases with increasing strain rate. It gives a higher strain rate sensitivity index values as compared to directionally solidified and as cast eutectic. At room temperature, strain rate sensitivity index (m) is less than 0.3 for all structures (directionally solidified, as cast, swaged and annealed). It suggests that at room temperature, primary deformation mechanism is based on movement of dislocations. At higher test temperatures (373 K, 423 K), interlamellar spacing does not affect the value of strain rate sensitivity index (m) (figs 4.17 & 4.19). The strain rate sensitivity index Vs strain rate curves for various directionally solidified specimens are nearly the same at higher temperatures. As discussed earlier, at higher temperatures, the strength of directionally solidified material can be evaluated by the rule of mixtures rather than by interlamellar spacing influence. The value of m for directionally solidified material remains the same with increasing strain rate at 373 K and 423 K.

As cast eutectic gives higher m values than directionally solidified material at higher temperatures but less than

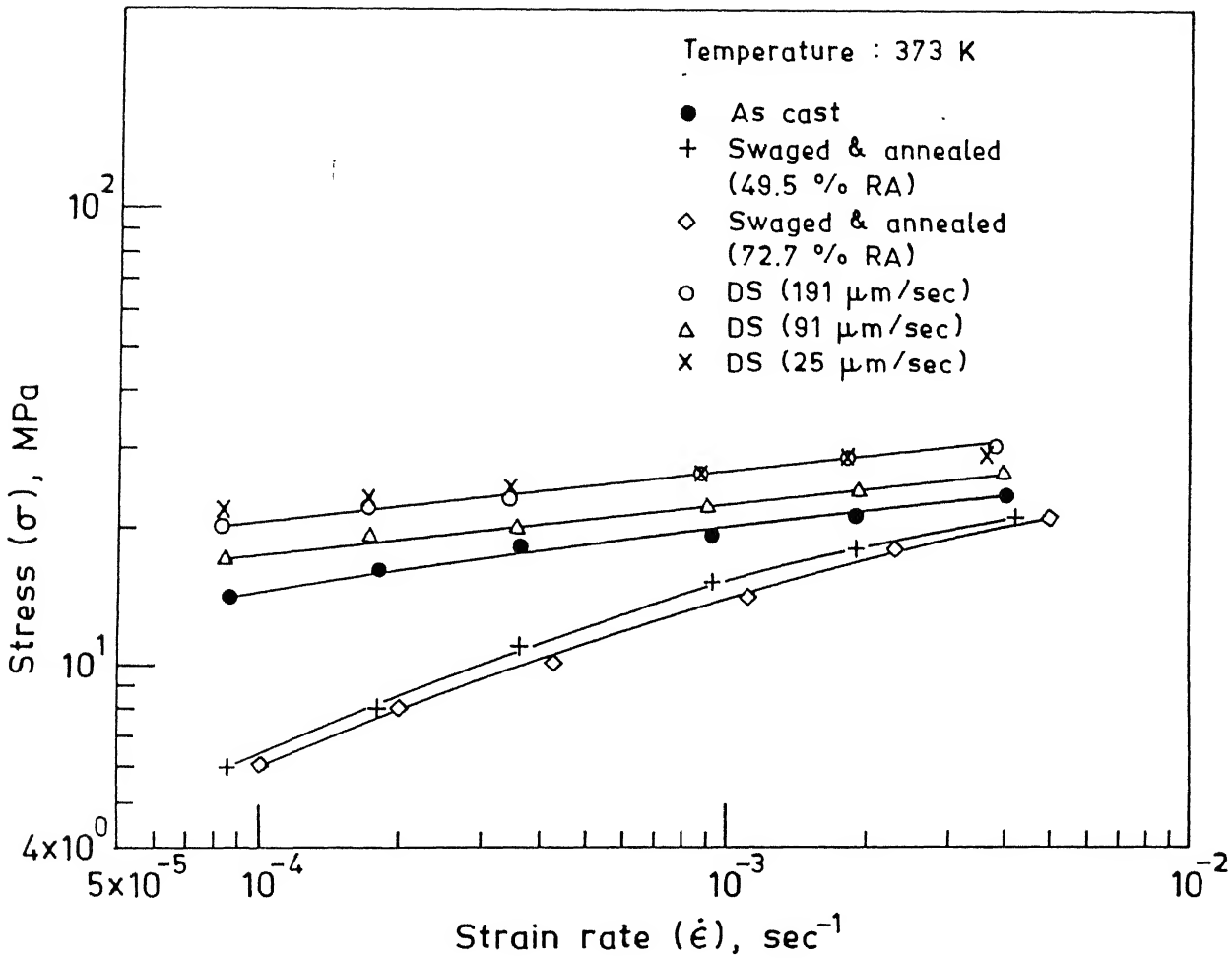

Fig. 4.16. Stress (σ) vs strain rate ($\dot{\epsilon}$) curves at 373 K. (DS = Directionally solidified)

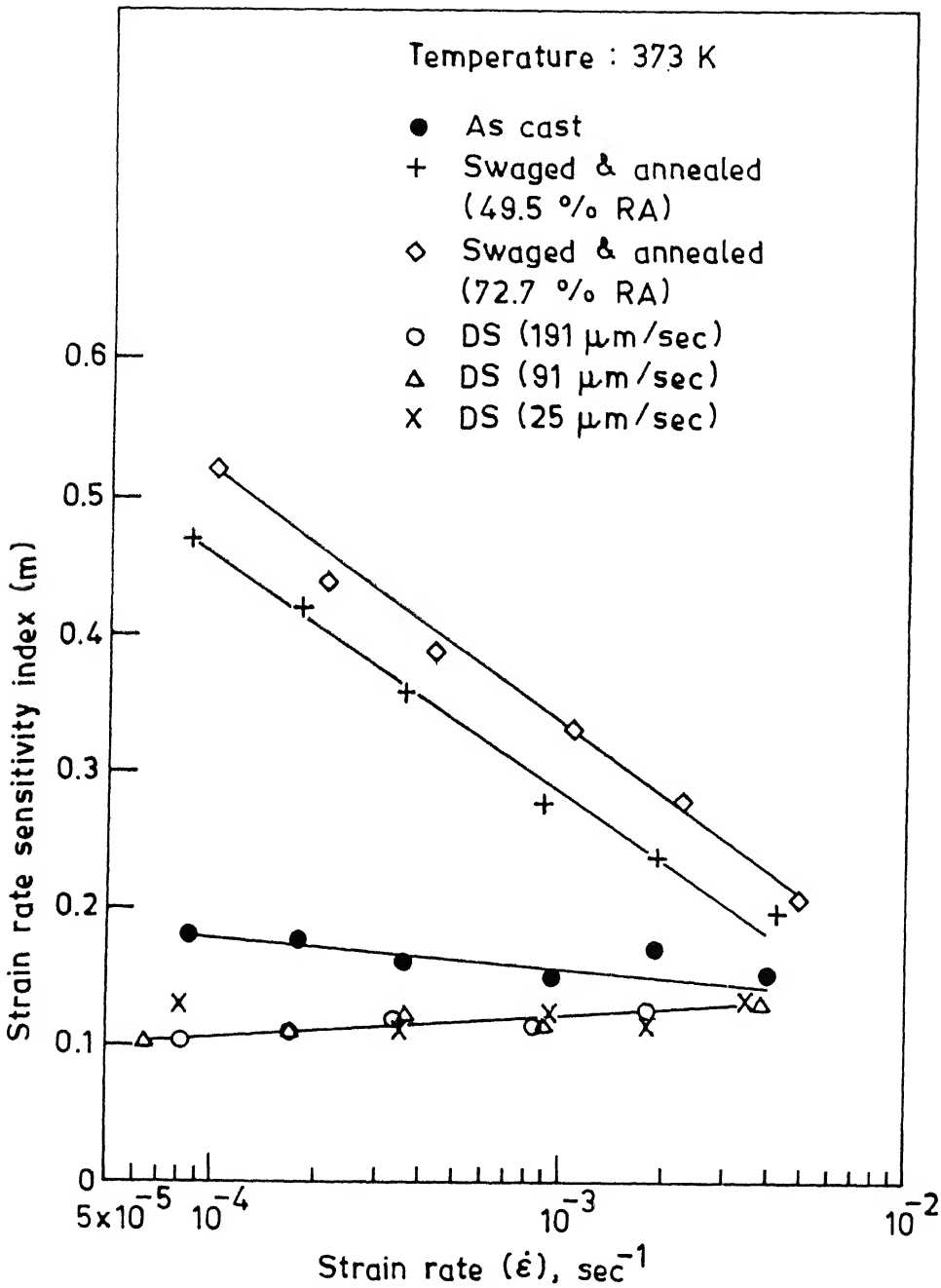

Fig. 4.17. Influence of strain rate ($\dot{\epsilon}$) on strain rate sensitivity index (m) at 373 K. (DS = Directionally solidified)

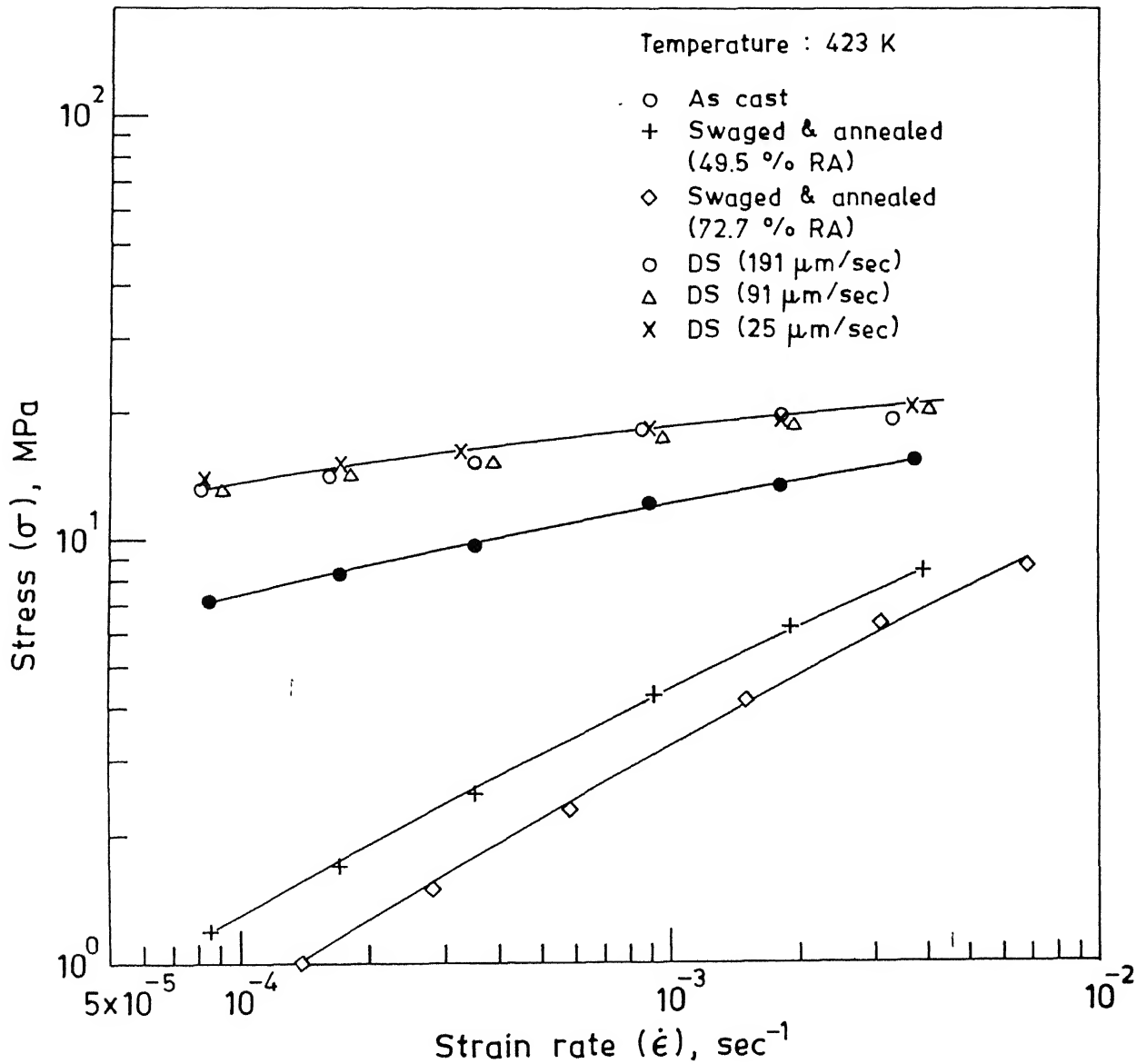

Fig. 4.18. Stress (σ) vs strain rate ($\dot{\epsilon}$) curves at 423 K. (DS = Directionally solidified)

that for swaged and annealed material. There is a slight decrease in the values for strain rate sensitivity index with increasing strain rate. The strain rate sensitivity index is less than 0.3 for as cast eutectic at 373 K and 423 K. This may be due to the microstructural details in as cast state where there is mixed type of microstructure with microsegregation and rough grain boundaries. In this case, the flow of material by grain boundary sliding becomes difficult.

At higher temperatures, swaged and annealed material gives high values of strain rate sensitivity index (>0.3). At 373 K, the m values are 0.5-0.6, while at 423 K, the m values are 0.6-0.7. The strain rate sensitivity index Vs strain rate curves for swaged and annealed material are closer to each other as there is not much difference in grain sizes of hot worked material with two different degrees of deformation. The higher 'm' values suggest that grain boundary sliding is the preferred mode of deformation in swaged and annealed material at higher temperatures. The microstructure of swaged and annealed material has a homogenised equiaxed structure with smooth grain boundaries which makes the grain boundary sliding easier. There is a transition in flow mechanism with increasing strain rate. At higher strain rates, deformation also takes place due to movement of dislocations. So there is a decrease in strain rate sensitivity with increasing strain rate. Figures 4.20 and 4.21 indicate the effect of temperature on strain rate sensitivity index Vs strain rate curves for directionally solidified eutectic and swaged and annealed eutectic respectively. There is a slight increase in strain

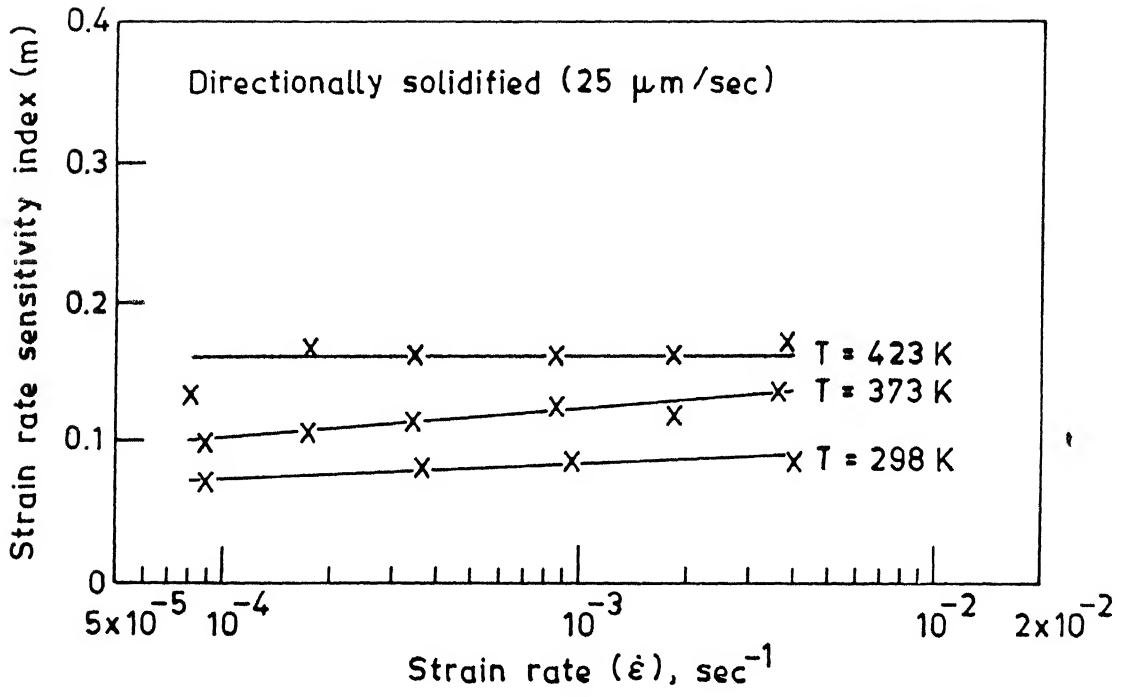

Fig. 4.20. Effect of temperature on strain rate ($\dot{\epsilon}$) vs strain rate sensitivity index (m) curves for directionally solidified lead-tin eutectic. Growth rate = 25 μm/sec.

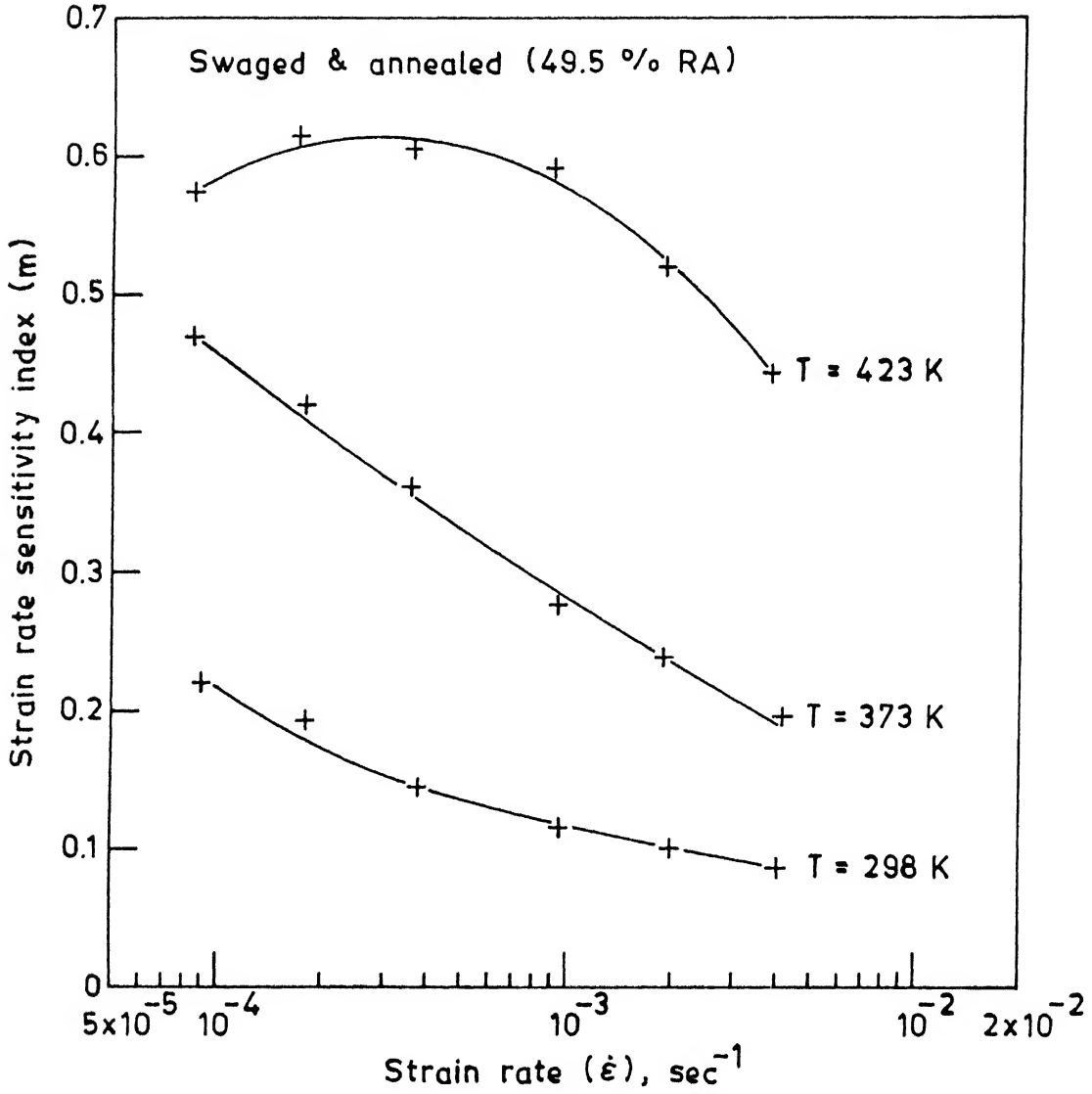

Fig. 4.21. Effect of temperature on strain rate ($\dot{\epsilon}$) vs strain rate sensitivity index (m) curves for swaged (49.5 % RA) and annealed eutectic.

rate sensitivity of directionally solidified eutectic at higher temperature while swaged and annealed eutectic has a marked influence of temperature on strain rate sensitivity. This is due to the fact that grain boundary sliding is not a mechanism for deformation of directionally solidified eutectic having lamellar structure, while swaged and annealed material with equiaxed structure deforms by grain boundary sliding at higher temperatures.

Figure 4.22 gives m vs $\dot{\epsilon}$ curves for pure lead and pure tin at two different test temperatures (298 K, 423 K). The strain rate sensitivity index (m) values are nearly same with increasing plastic strains at both the temperatures. The m values are less than 0.3 at 298 K and at 423 K for lead and tin. Accordingly the deformation mechanism is movement of dislocations rather than grain boundary sliding. Coarser grain sizes of lead and tin contribute to this effect.

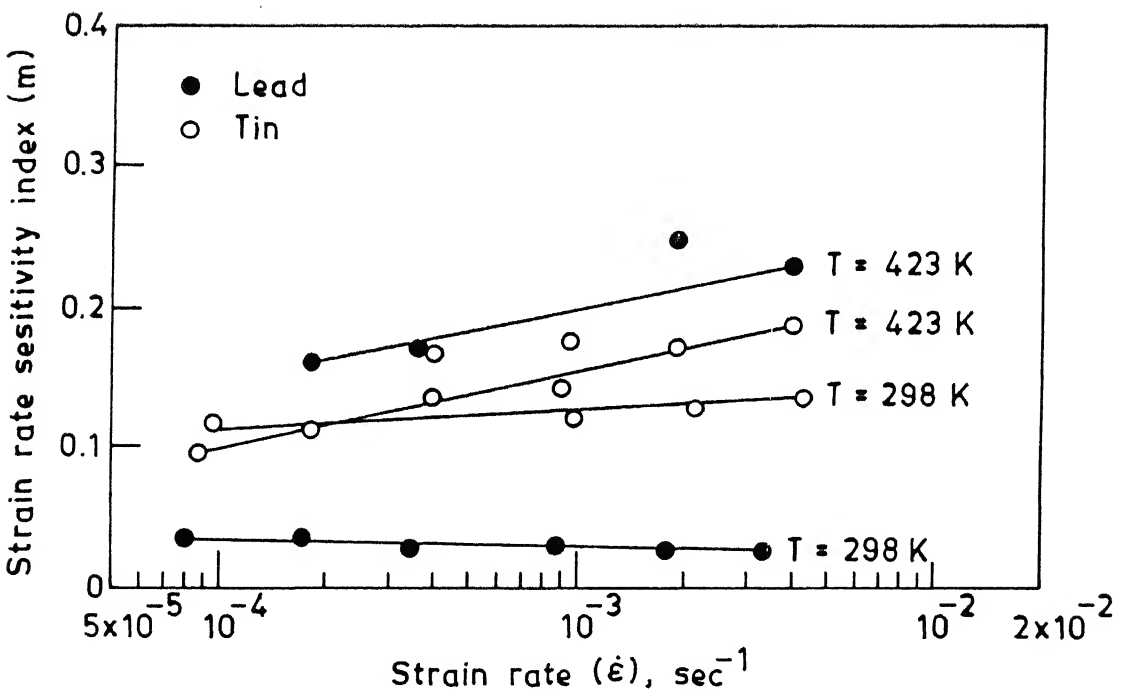

Fig. 4.22. Influence of strain rate ($\dot{\epsilon}$) on strain rate sensitivity index (m) for lead and tin .

5. SUMMARY AND CONCLUSIONS

The results and conclusions of the present study are summarised as follows:

1.At lowest speed of directional solidification (25 μm/sec), primary dendrites of tin rich phase were present in the microstructure. Presence of these primary dendrites is thought to be caused by the gravity segregation of lead at lowest speed of solidification which would have left the liquid with an off-eutectic composition.

2.Degeneracy in the structure has been observed in all speeds of directional solidification. Degeneracy has increased with increasing speed of directional solidification. At the highest speed (191 μm/sec), the structure was totally degenerate and showed no pockets of regular lamellar structure.

3.The data of this study do not seem to conform to the relation $\lambda^2 V$ = constant. It is expected to hold for a regular lamellar eutectic whereas in the present work, degeneracy in the structure has been observed at all speeds of directional solidification.

4.Room temperature compression test for directionally solidified eutectics show that the eutectic with the highest speed of solidification exhibits the best strength. Hall-petch type

relationship is applicable to the data of the present study at room temperature.

5.The extent of strain hardening observed at room temperature is maximum in directionally solidified structure, followed by as cast and swaged and annealed structure.

6.At higher test temperatures, strength of directionally solidified material with different speeds of solidification lie in a narrow band. The concept of rule of mixtures may be valid for this lamellar structure at higher temperature.

7.At all test temperatures, directionally solidified eutectic has shown more strength than as cast eutectic. Swaged and annealed eutectic has shown the lowest strength levels.

8.Increase in temperature decreases the strength levels for all types of microstructures. Drop in strength of directionally solidified eutectic with increasing temperature is smaller compared to as cast and hot worked structure.

9.In directionally solidified eutectic, softening was found to occur at lower plastic strains with increasing test temperatures. This may be due to the instability of lamellar structure because of higher degree of deformation at elevated temperatures.

10.At all test temperatures, flow stress vs strain rate

curves show that flow stress increases with increasing strain rate. The increase in flow stress for directionally solidified eutectic is less compared to as cast and swaged and annealed eutectic.

11.The strain rate sensitivity index (m) value is nearly the same and does not change with strain rate for all directionally solidified eutectics at any of the test temperatures. It shows that for directionally solidified eutectic, the mode of deformation is not the grain boundary sliding which has a higher rate sensitivity. Deformation is mainly due to direct dislocation mechanism. Directionally solidified eutectic shows less strain rate sensitivity compared to as cast and hot worked eutectic at all temperatures.

12.At room temperature test, strain rate sensitivity index (m) is less than 0.3 for all structures (directionally solidified, as cast, swaged and annealed).

13.As cast eutectic gives higher m values than directionally solidified material at higher temperatures but less than swaged and annealed material. The m values are less than 0.3 for as cast eutectic at all temperatures.

14.Swaged and annealed eutectic gives higher values of m at higher temperatures (0.5-0.6 at 373 K and 0.6-0.7 at 423 K). The higher m values show that grain boundary sliding is the

preferred mode of deformation. There is a transition in flow mechanism with increasing strain rate as there is a decrease in strain rate sensitivity with increasing strain rate.

REFERENCES

1. "Tin and Tin alloys", Metals hand book, ASM International, Vol 2, 8th edition, p.449.

2. M.C.Flemings, "Solidification prOcessing", McGraw Hill, (1976), p.93.

3. B.Chalmers, "Principles of solidification", John Willey & Sons, (1964), p.201.

4. K.A.Jackson and J.D.Hunt, Trans Met Soc. AIME, Vol 236 (1966), p1129.

5. R.M.Jordan and J.D.Hunt, Met Trans, Vol 2, (1971), p3401.

6. J.N.Clark and R.Elliot, Met Trans A, Vol 7A, (1976), p1197.

7. J.D.Livingston, H.E.Cline et al, Acta Metallurgica, Vol 18, (1970), p399.

8. H.E.Cline and J.D.Livingston, Trans Met Soc. AIME, Vol 245, (1969), p1987.

9. F.R.Mollard and M.C.Flemings, Trans Met Soc. AIME, Vol239, (1967), p1534.

10. M.C.Flemings, "Solidification Processing", McGraw Hill, (1976), p107.

11. J.D.Verhoeven, D.P.Mourer and E.D.Gibson, Met Trans A, Vol 8A, (1977), p1239.

12. J.D.Hunt, Ph.D Thesis, Cambridge University, Cambridge, (1963).

13. G.E.Dieter, "Mechanical Metallurgy", McGraw Hill, (1981), p329.

14. M.McLean, "Directionally Solidified Materials For High

Temperature Service", The Metals Society, (1983), p207.

15. L.J.Broutman, R.H.Krock, Editor K.G.Kreider, "Composite Materials", Academic Press, Vol 4, (1974), p101.

16. B.J.Shaw, Acta Metallurgica, Vol 15, (1967), p1169.

17. M.Sahoo et al, J of Mat. Science, Vol 15, (1980), p1097.

18. F.Vrunk et al, J of Mat. Science, Vol 15, (1980), p2573.

19. N.Furushiro and S.Hori, Scripta Metallurgica, Vol 13, (1979), p653.

20. B.P.Kashyap and G.S.Murty, Met Trans A, Vol 13 A, (1982), p53.

21 B.P.Kashyap and G.S.Murty, Mat. Science & Engg., Vol 50, (1981), p205.

22. A.E.Geckinli and C.R.Barrett, J of Mat. Science, Vol 11, (1976), p510.

23. P.Ravi Kumar, M.Tech Thesis, IIT Kanpur, (1991).

24. B.P.Kashyap, Ph.D Thesis, IIT Kanpur, (1979).

APPENDIX 1

Determination of the position of solid-liquid interface

The following method was adopted to precisely determine the position of the solid-liquid interface with reference to the bottom of the crucible containing the ingot. As shown in figure 3.4, the following fixed distances were measured before the run.

B -- Height of the cork arrangement above the top surface of the furnace.

C -- Total furnace length.

D -- Total thermocouple sheath length.

F -- Total length of the crucible stand.

K -- Distance from the lower surface of the chill holding ring to the furnace bottom.

After thermocouple sheath is adjusted such that it exactly touches the solid-liquid interface, the following variable distances have to be measured after equilibrium is attained in the system.

A -- The length of the thermocouple sheath that is visible above the cork arrangement.

H -- The length of the crucible stand from the lower surface of the chill holding ring to the base of the stand.

Let the solid-liquid interface be at any position after equilibrium is attained.

K + H -- Length of the crucible stand from furnace bottom to

its base.

{F - (K + H)} -- Length of the crucible stand that is projecting inside the furnace.

{D - (A + B)} -- Length of the thermocouple sheath inside the furnace.

So, [C -{D -(A + B)} - {F - (K + H)}] gives the exact height of the solid-liquid interface with respect to the bottom of the crucible.

APPENDIX 2

DETERMINATION OF FREEZING RATES DURING DIRECTIONAL SOLIDIFICATION RUN

RUN No. 1

POTENTIOMETER SETTING	CATHETOMETER READINGS INITIAL (CM)	FINAL (CM)	DISTANCE TRAVELLED (CM)	TIME TAKEN (S)	AVERAGE SPEED (u
	18.55	19	0.45	23.7	
	19.5	20	0.5	26.7	
5.06	21.3	22	0.7	36.3	191
	22.55	23.1	0.55	29.6	
	24	24.5	0.5	25	

RUN No. 2

POTENTIOMETER SETTING	CATHETOMETER READINGS INITIAL (CM)	FINAL (CM)	DISTANCE TRAVELLED (CM)	TIME TAKEN (S)	AVERAGE SPEED (u
	14.5	15.1	0.6	70.2	
	15.7	16.3	0.6	68	
	16.7	17	0.3	33.1	
	18.1	18.7	0.6	63.9	
5.02	19	19	0.5	56.6	91
	20	20.5	0.5	55	
	21	21.5	0.5	53	
	22	23	1	108.5	
	23.5	24	0.5	51	

RUN No. 3

POTENTIOMETER SETTING	CATHETOMETER READINGS INITIAL (CM)	FINAL (CM)	DISTANCE TRAVELLED (CM)	TIME TAKEN (S)	AVERAGE SPEED (cm/
	13.8	14.1	0.3	170.5	
	14.5	15	0.5	199	
	16	16.5	0.5	196.3	
	17	17.5	0.5	195	
4.98	18	18.5	0.5	185.5	25
	19	19.5	0.5	209.8	
	20	20.5	0.5	192.5	
	22.5	23	0.5	190.6	